JOURNAL OF PETROLOGY | VOLUME 52 | NUMBERS 7 & 8 | PAGES 1591–1617 | 2011 | doi:10.1093/petrology/egq029

Magmatic Evolution of the Giant El Teniente Cu–Mo Deposit, Central Chile

CHARLES R. STERN[1]*, M. ALEXANDRA SKEWES[1] AND ALEJANDRA ARÉVALO[2]

[1]DEPARTMENT OF GEOLOGICAL SCIENCES, UNIVERSITY OF COLORADO, BOULDER, CO 80309-0399, USA

[2]SUPERINTENDENCIA GEOLOGÍA, EL TENIENTE, CODELCO-CHILE, RANCAGUA, CHILE

RECEIVED JULY 7, 2009; ACCEPTED MAY 6, 2010
ADVANCE ACCESS PUBLICATION JUNE 28, 2010

El Teniente, the world's largest Cu deposit, is hosted in Late Miocene and Pliocene plutons that intrude the older Teniente Volcanic Complex (or Farellones Fm; 14·2–6·5 Ma). The Late Miocene and Pliocene plutonic host rocks of the deposit include, sequentially, the relatively large (>50 km^3) Teniente Mafic Complex laccolith (8·9 ± 1·4 Ma), the smaller (~30 km^3) Sewell equigranular tonalite complex (7·05 ± 0·14 Ma) and associated andesitic sills (8·2 ± 0·5 to 6·6 ± 0·4 Ma), small dacitic porphyry stocks (<1 km^3; 6·09 ± 0·18 Ma), the unusual Cu- and S-rich 'Porphyry A' anhydrite-bearing granitoid stock (<1 km^3; 5·67 ± 0·19 Ma), the Teniente Dacite Porphyry dike (<1 km^3; 5·28 ± 0·10 Ma), minor latite dikes (4·82 ± 0·09 Ma), and finally a small dacite intrusion (4·58 ± 0·10 Ma). These plutonic rocks are all isotopically similar to each other ($^{87}Sr/^{86}Sr$ = 0·7039–0·7042; ε_{Nd} = +2·5 to +3·5) and also to the Teniente Volcanic Complex extrusive rocks, but distinct from both older Late Oligocene to Early Miocene volcanic rocks ($^{87}Sr/^{86}Sr$ = 0·7033–0·7039; ε_{Nd} = +3·8 to + 6·2) and younger Pliocene post-mineralization mafic dikes and lavas ($^{87}Sr/^{86}Sr$ = 0·7041–0·7049; ε_{Nd} = +1·1 to −1·1). Multiple Cu-mineralized magmatic–hydrothermal breccia pipes were emplaced into these plutonic rocks during the same time period as the felsic porphyry intrusions, between at least 6·31 ± 0·03 and 4·42 ± 0·02 Ma. These mineralized breccia pipes, which formed by exsolution of magmatic fluids from cooling plutons, have their roots below the deepest level of mining and exploration drilling and were derived from the same magma chamber as the felsic porphyries, >4 km below the paleosurface. To produce the ~100 × 10^6 tonnes of Cu in the deposit requires a batholith-size (>600 km^3) amount of magma with ~100 ppm Cu. We suggest that both the mineralized magmatic–hydrothermal breccias and the progressively smaller volumes of more fractionated, but isotopically equivalent, Late Miocene and Pliocene felsic plutonic rocks that host the deposit were derived from the roof of a large, long-lived, thermally and chemically stratified, open-system magma chamber, or magmatic plumbing system, recharged from below by mantle-derived magmas. Only when this system fully solidified did post-mineralization mafic olivine-hornblende-lamprophyre dikes (3·85 ± 0·18 to 2·9 ± 0·6 Ma) pass through the system from the mantle to the surface. The significant progressive temporal isotopic evolution, to higher $^{87}Sr/^{86}Sr$ (from 0·7033 to 0·7049) and lower ε_{Nd} (from +6·2 to −1·1), that occurred between the Late Oligocene and Pliocene in the vicinity of El Teniente for mafic mantle-derived magmas, and by implication their sub-arc mantle-source region, was due in part to increased mantle-source region contamination by subducted crust tectonically eroded off the continental margin. The post-mineralization olivine-hornblende-lamprophyres also imply extensive hydration of the mantle below this portion of the Andean arc by the Pliocene, which may have played a role in producing oxidized volatile-rich magmas and mineralization at El Teniente.

KEY WORDS: *Chilean Andes; copper deposits; El Teniente; magmagenesis; petrochemistry*

INTRODUCTION

The giant El Teniente Cu–Mo deposit, located in central Chile (34°05′S, 70°21′W; Fig. 1), is the world's largest Cu deposit, originally containing ~100 million metric tonnes (Mt) of Cu (Skewes *et al.*, 2002, 2005). The deposit is

*Corresponding author. Telephone: 303-492-7170. Fax: 303-492-2606. E-mail: Charles.Stern@colorado.edu

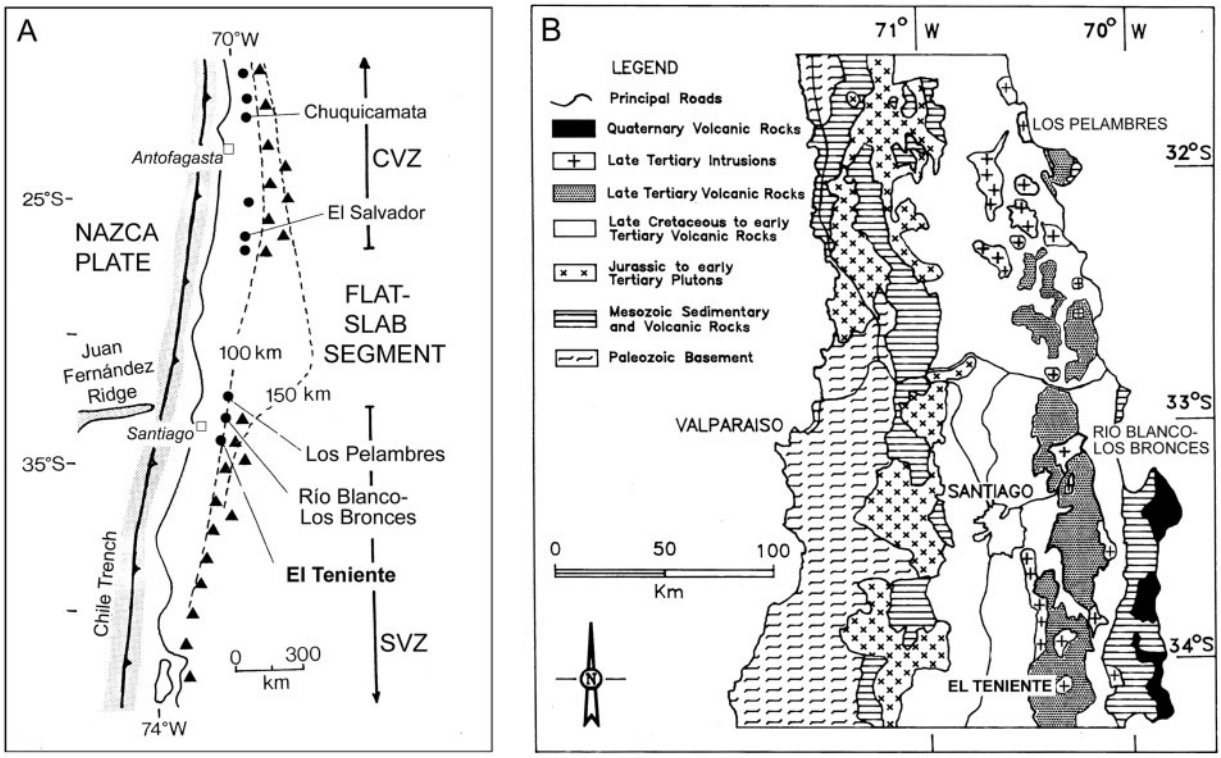

Fig. 1. Location maps of El Teniente and the two other giant Late Miocene and Pliocene Cu deposits in the Andes of central Chile, Los Pelambres and Río Blanco–Los Bronces, modified from Serrano *et al.* (1996). (a) Map showing tectonic features such as the location of the Chile Trench, which is the boundary between the Nazca and South American plates, and the depth in kilometers (100 and 150 km dashed lines) to the Benioff Zone below South America. The Cu deposits occur just east of the locus of subduction of the Juan Fernández Ridge. This also marks the boundary between the Andean Flat-Slab segment, below which the subduction angle is very low, as indicated by the depths to the upper boundary of the subducted slab, and the Southern Volcanic Zone (SVZ) of active volcanoes (▲), below which the subduction angle is steeper. The map also shows the location of the Central Volcanic Zone (CVZ) and some of the Late Eocene and Early Oligocene Cu deposits in northern Chile. (b) Simplified regional geology of central Chile. In this schematic map, both the Coya-Machali (Abanico) and Farellones Formations are included together in the belt of Late Tertiary volcanic rocks.

hosted in Late Miocene and Pliocene igneous rocks (Figs 2 and 3). The chronology of the formation of these igneous rocks, both in and around the deposit, is reasonably well determined (Fig. 4; Cuadra, 1986; Kurtz *et al.*, 1997; Maksaev *et al.*, 2004), and the published petrochemical database for understanding the regional magmatic evolution at the latitude of El Teniente is among the most detailed in the southern Andes (Stern & Skewes, 1995; Nystrom *et al.*, 2003; Kay *et al.*, 2005; Muñoz *et al.*, 2006).

However, the petrochemistry and genesis of the igneous rocks within the El Teniente deposit have received less attention than those surrounding the deposit. It is clear, from the overlap of the isotopic ages of both the igneous rocks ($8{\cdot}9 \pm 1{\cdot}4$ to $4{\cdot}58 \pm 0{\cdot}10$ Ma; Fig. 4) and the multiple alteration and mineralization events in the deposit ($6{\cdot}31 \pm 0{\cdot}03$ to $4{\cdot}42 \pm 0{\cdot}02$ Ma), that there is a direct genetic relation between igneous activity and mineralization. This was originally recognized by Lindgren & Bastin (1922), who identified several periods of intrusion and mineralization at El Teniente, and concluded that this deposit 'preserves a record of alternating igneous activity and ore deposition that affords convincing evidence of the intimate genetic connection between igneous rocks and ore deposits'. As a contribution to the understanding of this genetic connection, we present the results of a petrochemical study of the igneous rocks within the El Teniente deposit.

GEOLOGICAL BACKGROUND

El Teniente, along with Los Pelambres (32°S; >25 Mt of Cu; Atkinson *et al.*, 1996) and Río Blanco–Los Bronces (33°S; >50 Mt of Cu; Warnaars *et al.*, 1985; Serrano *et al.*, 1996; Frikken *et al.*, 2005), formed during Miocene and Pliocene times in the Andes of central Chile (Fig. 1), and are among the youngest and largest Cu–Mo deposits in the Andes. They are copper-, sulfur-, iron-, calcium-, molybdenum- and boron-rich, but gold-poor deposits that share important features. These include their large tonnage and high hypogene copper grade, and the fact that most of the copper mineralization occurs as primary hypogene

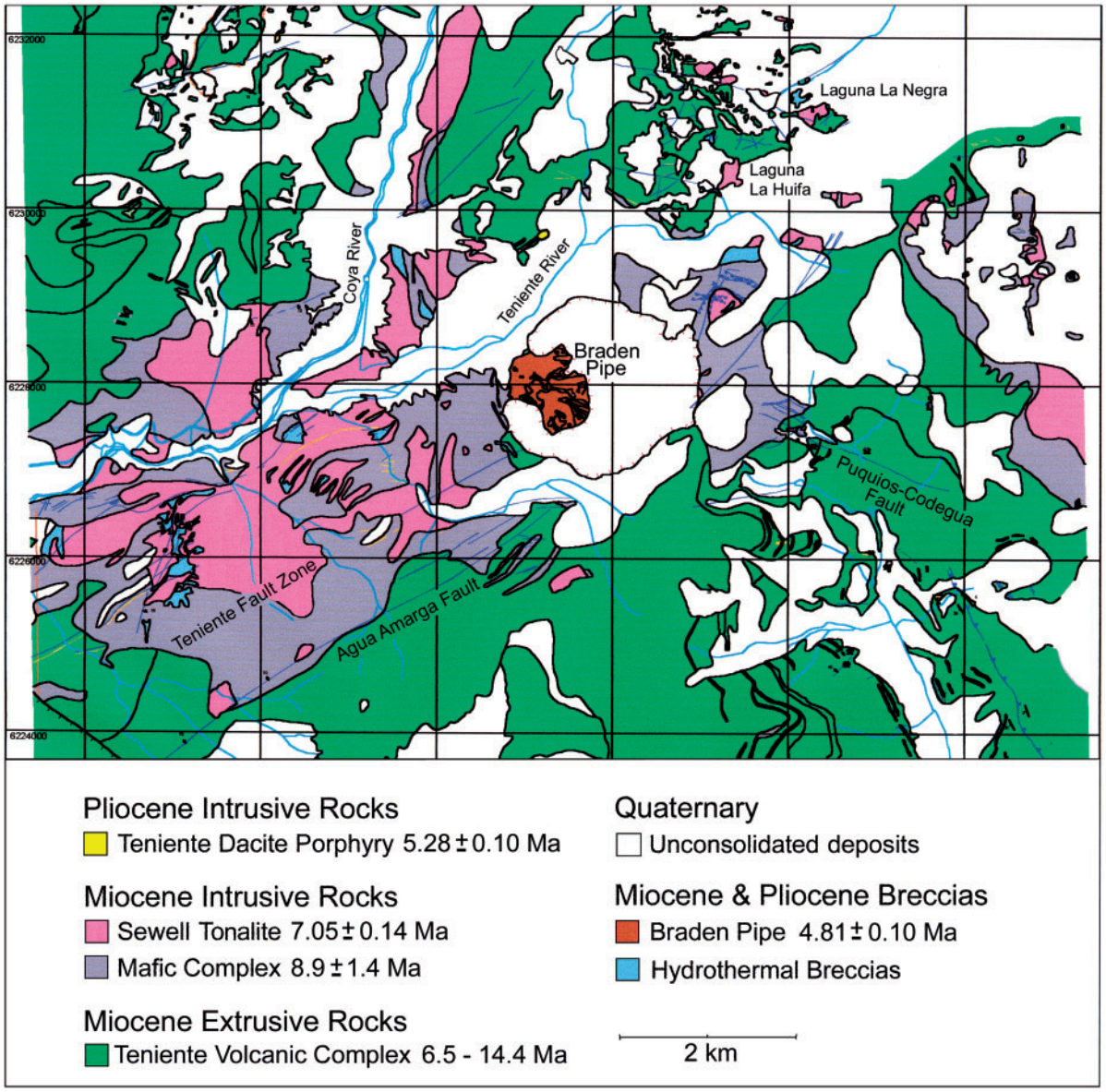

Fig. 2. Geological map of the area surrounding the El Teniente copper deposit, modified from Morel & Spröhnle (1992) and Skewes *et al.* (2002, 2005). The Braden breccia pipe is located at the intersection of the Teniente Fault Zone, which trends NE–SW between the Teniente River and Agua Amarga fault, and the NW–SE-trending Puquios–Codegua fault.

ore. Another distinctive feature that each of these three deposits has in common is the presence of large magmatic–hydrothermal breccias, both mineralized and unmineralized (Skewes & Stern, 1994, 1995, 1996). The genesis of these magmatic–hydrothermal breccias has been attributed to the exsolution of high-temperature magmatic fluids from cooling plutons (Warnaars *et al.*, 1985; Skewes & Stern, 1994, 1995, 1996; Vargas *et al.*, 1999; Skewes *et al.*, 2002, 2003).

The three deposits in central Chile occur across the boundary between two major Andean tectonic segments (Fig. 1a): the Flat-Slab segment to the north, below which the angle of subduction has decreased significantly since the Miocene and where volcanism is now absent, and the Southern Volcanic Zone (SVZ), below which the subduction angle is steeper and volcanism is active. The formation of the three deposits is closely associated in time with the changing geometry of subduction that has produced this segmentation of the Andes (Stern, 1989, 2004; Skewes & Stern, 1994, 1995; Stern & Skewes, 1995, 2005; Rosenbaum *et al.*, 2005). As with the older copper deposits in northern Chile, such as Chuquicamata and El Salvador (Fig. 1a),

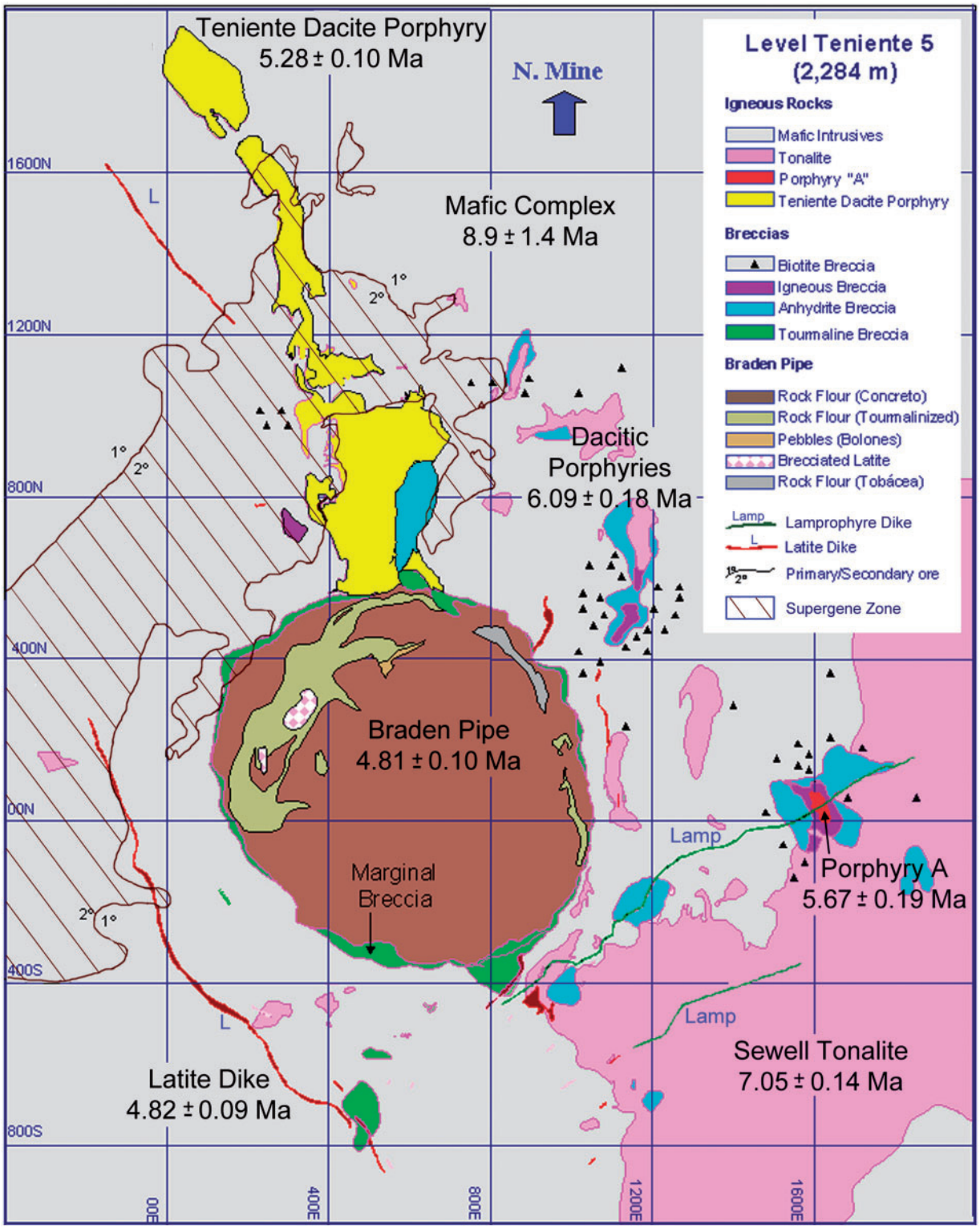

Fig. 3. Geological map of level Teniente 5 (2284 m above sea level) in the mine, modified from Skewes *et al.* (2002, 2005). The Dacitic Porphyries, north of the Sewell Tonalite, are mapped as a distal portion of this pluton, although they are younger (Maksaev *et al.*, 2004) and have an independent origin (Guzmán, 1991; Hitschfeld, 2006). The spatial extent of biotite breccias is projected onto this level from where they have been mapped between levels Teniente 4 and 8.

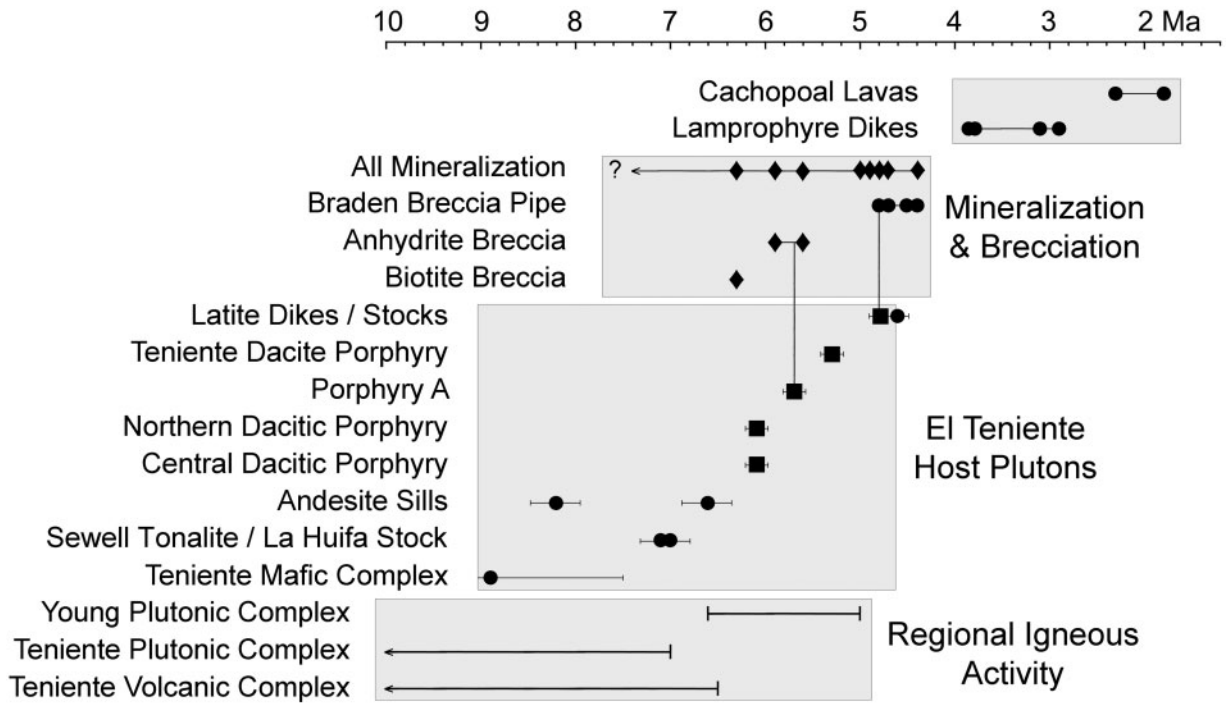

Fig. 4. Schematic chronology of the ages of the Late Miocene and Pliocene volcanic and plutonic host rocks of the El Teniente deposit, including both K–Ar mineral and whole-rock ages (●) and U–Pb in zircon ages (■), as well as Re–Os ages of mineralization (♦) and the ages of breccias determined either from Re–Os of molybdenite within the breccia matrix mineral assemblage or, in the case of the Braden Pipe, from K–Ar of sericite formed by alteration of clasts and wall-rock during breccia emplacement. Vertical lines connect igneous rocks with contemporaneous breccias. Horizontal lines indicate range of ages for regional units and uncertainties for specific rocks. Sources of data are Cuadra (1986), Maksaev *et al.* (2004), Cannell *et al.* (2005) and Kay *et al.* (2005). Skewes & Stern (2007) and Stern *et al.* (2007) discussed uncertainties in the complete published dataset and the cross-cutting field relations that provide the basis for the selection of ages in this figure.

copper mineralization occurred during a relatively restricted time interval (~3 Myr; Fig. 4), at the end of a more extended period of magmatic activity (>10 Myr), just prior to the eastward migration of the locus of the Andean volcanic arc (Maksaev & Zentilli, 1988; Cornejo *et al.*, 1997). Eastward migration of the magmatic arc occurred in central Chile during the Late Miocene and Pliocene, as the angle of subduction decreased (Stern, 1989, 2004; Stern & Skewes, 1995, 2005; Kay *et al.*, 2005). As the subduction angle decreased, beginning in the Middle Miocene, the crust in central Chile was deformed and thickened (Godoy *et al.*, 1999; Giambiagi *et al.*, 2001; Giambiagi & Ramos, 2002), and uplifted and eroded (Skewes & Holmgren, 1993; Kurtz *et al.*, 1997; Kay *et al.*, 2005).

The first comprehensive geological description of El Teniente was that of Lindgren & Bastin (1922). They described this deposit as hosted in a sill, formed of andesite porphyry and quartz diorite, which was intruded into a thick pile of volcanic rocks. Cuadra (1986) presented a basic chronology of the development of the deposit based on K–Ar dates on extrusive and intrusive igneous rocks, breccias and alteration events in and surrounding the El Teniente mine. He concluded that the Miocene extrusive rocks of the Farellones Formation in the vicinity of El Teniente ranged in age from 14 to 8 Ma, and felsic intrusive rocks within the deposit from 7·4 to 4·6 Ma. Recently determined U–Pb in zircon ages for the igneous rocks in the deposit (Maksaev *et al.*, 2004), and Re–Os mineralization ages of molybdenite (Maksaev *et al.*, 2004; Cannell *et al.*, 2005), are summarized in Fig. 4.

METHODS

Samples were collected from both surface localities around the mine, and from drill core within the hypogene zone of the mine. Table 1 and Table 1ES in the Electronic Supplement (available for downloading at http://www.petrology.oxfordjournals.org/) list primary igneous minerals and alteration phases for each sample analyzed, as well as the intensity of alteration. This ranges from weak (fresh plagioclase, some mafic minerals preserved, and igneous texture intact) to strong (plagioclase partially altered, mafic phases replaced, and igneous textures partially to totally obliterated). Petrological descriptions of each rock unit sampled are presented in the Electronic Supplement.

Table 1: Sample locations, textures and rock names, and primary igneous and secondary alteration mineralogy

Sample or	Location*			Igneous features		Alteration	
DDH no.	N or S	E or W	Elevation (m)	Texture/rock	Igneous minerals	Intensity	Secondary minerals
Mafic intrusive rocks inside the mine (CMET; 8·9 ± 1·4 Ma)							
DDH540-2082′	607N	1358E	1766	Gabbro	Pl, Cpx, r-Maf	Moderate	Chl, Act, Bt
DDH1411-1630′	565S	430E	1910	Gabbro	Pl(An8–55), r-Px, r-Ol(?)	Moderate	Bt, Chl
Mafic sills outside the mine (CMET; 8·9 ± 1·4 Ma)							
EX2004-4	34·093S	70·443W	Surface	Porph basalt	Pl(An77–51), Ol(Fo74), Cpx, Ti-Mag	Fresh	
QT-4	6·232·000N	376·000E	Surface	Diabase	Pl	Strong	Chl, Ep, Cal
AS-99-1C	34·097S	70·424W	Surface	Porph basalt	Pl(An51–40), Bt, Mag, r-Px, Fe–Ti Ox	Weak	Chl
Cerro Montura andesitic sills (8·2 ± 0·5 and 6·6 ± 0·4Ma)							
TTc9	6·229·640N	366·730E	Surface	Andesite	Pl(An62–50), Opx, Am, Fe–Ti Ox	Fresh	
TTc10	6·227·900N	364·600E	Surface	Andesite	Pl(An46–43), Hb, Cpx	Fresh	
Sewell Tonalite (7·05 ± 0·14 Ma)							
400S/1780E	400S	1780E	2165	Tonalite	Pl. Bt, r-Am, Qtz	Weak	Act, Chl, Bt, Ttn, Ep, Mag
Ttc5	130N	1770E	2284	Tonalite	Pl(An34–15), Bt, r-Maf, Qtz	Moderate	Chl, Ep
Northern Dacite Porphyry (6·11 ± 0·13 Ma)							
DDH2370-159	990N	1000E	1920	Dacitic porph	Pl(An30–19), r-Am, Qtz	Strong	Qtz, Chl, Ser, Cal
Central Dacite Porphyry (6·08 ± 0·22 Ma)							
DDH1824-655′	314N	1340E	2180	Dacitic porph	Pl, Bt, r-Maf	Strong	Qtz, Ser, Cal
Porphyry A (5·67 ± 0·19 Ma)							
DDH1446-266′	10N	1650E	2220	‘Microdiorite’	Pl(An7), K-feld, Qtz, Anh, Bt	Weak	Chl, Ser
DDH1473-970′	100N	1650E	2000	‘Andesite’	Pl(An32), Bt, Qtz, Anh	Weak	
Teniente Dacite Porphyry (PDT; 5·28 ± 0·10 Ma)							
DDH1134-79′	1012N	520E	2145	Porph dacite	Pl(An24–7), Bt, Qtz, Anh	Weak	Bt, Ser
DDH1134-302′	1010N	445E	2116	Porph dacite	Pl(An27–7), Bt, r-Am, Qtz	Weak	Ser, Chl, Cal
DDH1134-365′	1006N	437E	2105	Porph dacite	Pl(An24–7), Bt, r-Maf, Qtz, K-feld, Anh	Weak	Chl, Cal, Ser, Anh
Latite dikes (4·82 ± 0·09 Ma)							
DD1394-92′	414S	430E	2270	Porph latite	Pl(An26–8), r-Maf	Moderate	Ser, Chl, Cal, Anh

And, andesite; Bas, basalt; Porph, porphyry; Ac, actinolite; Am, amphibole; Anh, anhydrite; Bt, biotite; Cal, calcite; Chl, chlorite; Cpx, clinopyroxene; En, enstatite; Ep, epidote; Hbl, hornblende; Hem, hematite; Idd, iddingsite; K-feld, potassium feldspar; Maf, mafic mineral; Mag, magnetite; Ol, olivine; Opx, orthopyroxene; Or, orthoclase; Ox, oxides; Pl, plagioclase; Px, pyroxene; Qtz, quartz; Ser, sericite; Ttn, titanite; Tur, tourmaline; r, replaced; Weak, plagioclase fresh, some mafic minerals preserved, texture intact; Moderate, plagioclase preserved, mafic minerals replaced, texture preserved; Strong, plagioclase can be altered, mafic minerals replaced, partial to total destruction of texture.
*Locations inside the mine are given in mine coordinates (Fig. 3). Locations outside the mine are given in UTM or degrees latitude.

Samples were selected from areas of low vein density and all visible veins were removed from them prior to analysis. In their study of volcanic and plutonic rocks from the Teniente area, Kay *et al.* (2005) concluded that hydrothermal alteration may have affected loss on ignition (LOI), K_2O, Na_2O, Rb, Cs and Ba, but that even strong alteration has not affected the immobile element [rare earth element (REE), Sr, U, Th, Hf, Nb and Y] chemistry. Our discussion of the petrogenesis of the rocks focuses on constraints provided by these immobile elements and isotopic data that were obtained only for the freshest, least altered samples.

Major- and trace-element compositions (Tables 2 and 3, and Tables 2ES–6ES in the Electronic Supplement) were determined by Actlabs. The Sr and Nd isotopic (Table 4) compositions of 17 selected samples were determined by solid-source mass-spectrometry techniques (Farmer *et al.*, 1991) at the University of Colorado. Mineral compositions were determined using a JEOL electron microprobe at the University of Colorado.

IGNEOUS ROCKS

Crystalline basement

Paleozoic igneous and metamorphic rocks occur both well to the west of El Teniente, along the Pacific coast (Fig. 1b), and also to the east, in the High Andean Cordillera along the drainage divide between Chile and Argentina. The Paleozoic basement west of El Teniente is intruded by Mesozoic plutonic rocks. These older metamorphic and igneous rocks may occur in the deep crust below El Teniente, but they do not crop out within the mine or in the immediate vicinity surrounding the deposit (Figs 2 and 3).

Tertiary volcanic rocks

El Teniente is located in a belt of Middle to Late Miocene extrusive and intrusive igneous rocks (Fig. 1b), which are part of the Farellones Formation (Fig. 2). Extrusive rocks of the Farellones Formation overlie older continental volcanic rocks, up to 3300 m thick, of the Oligocene to Early Miocene Coya-Machalí (or Abanico) Formation (>15 Ma; Charrier *et al.*, 2002; Muñoz *et al.*, 2006; Montecinos *et al.*, 2008), which were initially uplifted and deformed beginning in the Early Miocene (19–16 Ma; Kurtz *et al.*, 1997; Kay *et al.*, 2005), and again more strongly in the Late Miocene and Pliocene (9–3·5 Ma; Godoy *et al.*, 1999). Mafic Coya-Machalí (or Abanico) Formation volcanic rocks were formed below thin (<30 km) crust, or in a transtensional intra-arc basin (Godoy *et al.*, 1999), by relatively high degrees of partial melting of sub-arc mantle modified to a small degree by the influx from below of slab-derived components (Nystrom *et al.*, 2003; Kay *et al.*, 2005; Muñoz *et al.*, 2006). This is indicated by their low La/Yb ratios (2·3–5·6), as well as their initial $^{87}Sr/^{86}Sr$ (0·7033–0·7039) and ε_{Nd} (+3·8 to + 6·2; Figs 5 and 6). Although the Coya-Machalí (Abanico) Formation volcanic rocks do not crop out either within or in the immediate vicinity of the El Teniente deposit (Figs 2 and 3), these rocks occur both to the west and the east of the deposit, and they almost certainly also occur at depth below the deposit.

Extrusive rocks of the Miocene Farellones Formation, locally referred to as the Teniente Volcanic Complex (Kay *et al.*, 2005), are the oldest rocks exposed in the immediate area surrounding the deposit (Fig. 2). The Farellones Formation is a sequence of >2500 m of lavas, volcanoclastic rocks, dikes, sills and stocks of basaltic to rhyolitic composition (Vergara *et al.*, 1988; Rivano *et al.*, 1990). The Teniente Volcanic Complex near the deposit has been correlated with the upper part of this formation and dated between 14·4 and 6·5 Ma (Cuadra, 1986; Vergara *et al.*, 1988; Kay *et al.*, 2005). No extrusive rocks with ages less than 6·5 Ma have been found in the vicinity of the El Teniente deposit.

The extrusive rocks of the Teniente Volcanic Complex were intruded by gabbro, diabase, diorite, tonalite, latite, and dacite porphyry plutons between 12·3 and 4·6 Ma (Cuadra, 1986; Kurtz *et al.*, 1997; Maksaev *et al.*, 2004; Kay *et al.*, 2005). Kurtz *et al.* (1997) and Kay *et al.* (2005) divided these intrusive rocks into the Teniente Plutonic Complex (12·3–7·0 Ma) and the Younger Plutonic Complex (6·6 to ~5 Ma), the latter emplaced after cessation of volcanic activity in the region (Fig. 4). As discussed below in more detail, the emplacement of the plutonic rocks within the El Teniente deposit spans the range from $8·9 \pm 1·4$ to $4·58 \pm 0·10$ Ma, and therefore, from an age perspective, they correspond to both the Teniente and the Younger Plutonic Complex rocks.

The Teniente Volcanic Complex consists of tholeiitic to calc-alkaline extrusive rocks, which plot in the medium- to high-K group of convergent plate boundary arc magmas (Kay *et al.*, 2005). Mafic rocks of the Teniente Volcanic Complex generally have higher La/Yb (4·4–9·2) compared with rocks of the older Coya Machalí Formation (Kay *et al.*, 2005), and mafic, intermediate and silicic rocks also have higher initial $^{87}Sr/^{86}Sr$ (0·7039–0·7041) and lower initial ε_{Nd} (+2·7 to + 3·6; Figs 5 and 6). These differences are interpreted to represent a change from magma genesis below and within relatively thin continental crust during the mid-Tertiary, when the Coya Machalí Formation was generated, to conditions of thickened continental crust when the Teniente Volcanic Complex formed in the Middle to Late Miocene.

Teniente Plutonic Complex rocks have isotopic compositions similar to Teniente Volcanic Complex extrusive rocks, whereas Younger Plutonic Complex felsic granitoids have higher $^{87}Sr/^{86}Sr$ (0·70424–0·70441) and lower ε_{Nd} (+0·74 to −0·08; Kurtz *et al.*, 1997; Kay *et al.*, 2005). However, as discussed below, the felsic plutonic rocks

Table 2: Major- and trace-element compositions of samples of CMET, Sewell Tonalite and andesite sills

	CMET inside mine		CMET outside mine			Andesite sills		Sewell Tonalite	
Sample:	540-2082′	1411-1630′	EX2004-04	QT-4	AS-99-1C	TTc9	TTc10	400S/1780E	TTc5
SiO_2	51·30	51·08	51·94	49·65	59·78	60·90	61·50	62·05	63·70
TiO_2	1·07	1·09	0·92	1·00	0·74	0·75	0·77	0·57	0·39
Al_2O_3	18·68	17·07	18·19	17·96	17·67	16·80	16·90	18·38	17·10
Fe_2O_3	9·89	11·04			3·50	3·90	3·60	1·71	1·90
FeO			8·78	9·90	3·46	2·20	1·90	1·72	2·40
MnO	0·15	0·08	0·13	0·53	0·20	0·10	0·08	0·07	0·08
MgO	5·23	5·75	5·71	5·29	1·72	2·80	2·60	1·58	1·50
CaO	9·00	6·58	7·87	6·56	4·12	5·60	5·70	4·41	3·90
Na_2O	3·21	2·15	3·82	4·30	3·97	4·38	4·54	5·98	4·93
K_2O	1·00	2·56	1·01	1·03	2·05	2·50	2·50	1·47	2·20
P_2O_5	0·22	0·19	0·2	0·22	0·2	0·20	0·22	0·19	0·21
LOI	1·07	1·46	0·98	4·53	2·4	0·94	0·60	1·50	1·80
Total	100·82	99·05	99·55	100·97	99·80	101·07	101·00	99·73	100·17
Cs	5·3	18	7	0·8	11·7	2·8	3·8	7·4	6·1
Rb	54	159	26	29	73	82	74	60	96
Sr	535	383	468	595	547	543	700	946	699
Ba	158	100	235	310	517	539	504	501	528
La	9·2	11·4	13·4	11·5	15·8	19·1	16·7	16·4	14·4
Ce	20·3	26·4	30·3	26·5	34·0	44·9	38·8	33·3	34·7
Pr	2·80	3·40	3·72	3·20	4·22			4·32	3·97
Nd	13·3	15·5	16·6	15·8	18·9	25·0	21·9	16·2	19·2
Sm	3·30	3·71	4·00	3·90	3·80	5·13	4·26	2·90	3·39
Eu	1·29	1·04	1·22	1·16	1·05	1·18	1·00	0·88	0·88
Gd	3·50	3·11	3·70	3·40	3·40			1·90	2·90
Tb	0·60	0·51	0·60	0·60	0·50	0·60	0·41	0·20	0·29
Dy	3·30	3·00	3·40	3·30	3·10			1·00	1·80
Ho	0·60	0·60	0·70	0·70	0·60			0·20	0·30
Er	1·90	1·60	1·90	2·00	1·80			0·50	0·90
Tm	0·30	0·24	0·28	0·27	0·25			0·07	0·12
Yb	1·70	1·48	1·70	1·60	1·50	2·03	1·27	0·40	0·92
Lu	0·24	0·21	0·25	0·25	0·22	0·26	0·16	0·06	0·11
Y	17	15	15	17	18	21	15	6	11
Zr	73	56	86	74	164	158	133	104	94
Hf	1·9	1·7	2·7	2·5	4·9	4·8	4·3	2·7	3·2
Th	1·3	1·2	3·7	2·9	11·1	9	7·9	1·7	4·3
Sc	27	30	21	24	14	15	12	6	6
Cr	263	292	268	41				50	24
Ni	75	198	134	30				<20	<20
Cu	204	1325	115	20	125			250	480
S	700	11120	400	200	300			400	
La/Yb	5·4	7·7	7·9	7·2	10·5	9·4	13·1	41·0	15·6
Dy/Yb	1·94	2·00	2·00	2·06	2·07			2·5	1·96
Sr/Y	33	26	31	35	30	26	36	157	63

Table 3: Major- and trace-element compositions of samples of felsic intrusive rocks

	Dacitic porphyries		Porphyry A		Teniente Dacite Porphyry		Latite dike	
Sample:	2370-159	1824-655′	1473-970′	1446-266	1300-403′	1134-302′	1134-79′	1394-92′
SiO_2	63·96	62·90	48·45	56·34	66·26	64·42	59·89	60·93
TiO_2	0·38	0·43	1·01	0·42	0·38	0·53	0·61	0·63
Al_2O_3	16·30	16·16	18·62	13·86	16·85	17·76	16·73	17·24
Fe_2O_3	2·57	1·43	7·54	2·74	1·83	0·9	1·70	2·14
MnO	0·04	0·04	0·03	0·02	0·02	0	0·01	0·02
MgO	1·08	0·89	4·73	1·41	1·01	1·02	2·22	1·86
CaO	2·70	2·74	5·73	6·72	2·82	3·69	4·77	4·61
Na_2O	5·19	3·84	4·33	3·80	5·53	6·8	5·55	4·76
K_2O	3·11	5·98	3·63	5·68	2·64	2·67	2·93	2·23
P_2O_5	0·14	0·14	0·22	0·17	0·14	0·2	0·17	0·21
S			1·44	3·35				
LOI	3·44	4·89	4·66	7·99	1·95	3·35	4·83	5·74
Total	98·91	99·45	100·39	102·49	99·43	101·34	99·40	100·37
Cs	7·0	2·9	16·3	5·3	1·5	3·9	3·9	2·7
Rb	124	142	209	187	66·7	54·6	87	80·5
Sr	568	415	499	456	699	823	680	742
Ba	564	815	244	601	644	464	762	311
La	12·8	13·3	10·6	24·1	10·4	15·15	13·9	14·6
Ce	24·3	24·0	21·4	53·7	20·1	30·74	27·9	30·9
Pr	2·66	2·47	2·84	6·29	2·42	3·92	3·68	4·00
Nd	10·2	7·40	13·43	26·12	9·0	15·11	14·1	15·3
Sm	1·83	1·00	3·44	4·63	1·58	2·51	2·80	2·80
Eu	0·63	0·36	1·00	0·79	0·65	0·69	0·78	0·83
Gd	1·26	0·60	2·96	3·17	1·40	1·90	2·20	2·30
Tb	0·16		0·51	0·38	0·20	0·17	0·30	0·20
Dy	0·82	0·40	2·69	1·89	0·80	0·76	1·50	1·00
Ho	0·15		0·50	0·34	0·18	0·13	0·30	0·20
Er	0·43	0·20	1·39	0·94	0·50	0·35	0·80	0·50
Tm	0·06		0·19	0·13	0·07	0·04	0·12	0·07
Yb	0·42	0·30	1·12	0·79	0·40	0·28	0·80	0·40
Lu	0·07	0·04	0·16	0·11	0·06	0·05	0·11	0·07
Y	6	3	13	9	5	4	8	6
Zr	96	95	95	81	94	95	90	108
Hf	2·8	2·7	2·8	3·9	2·4	2·6	2·5	2·9
Th	3·4	2·8	0·8	5·9	2·8	2·7	2·6	2·3
Sc	4	3	21	2·6	4	4	9	8
Cr	<20	<20	<20	<20	11	58	40	42
Ni	<20	<20	<20	<20	34	78	<20	86
Cu	2210	2520	899	2380	6000	2410	310	1250
S	7300	6500	14400	33500	9200	8600	2800	1420
La/Yb	30·8	44·3	9·5	30·5	23·7	54·1	17·3	36·5
Dy/Yb	2		2·5	2·4	2	2·4	1·88	2·25
Sr/Y	95	140	37	51	160	206	85	124

Table 4: Sr and Nd isotopic compositions of igneous rocks associated with El Teniente Cu–Mo deposit

Sample no.	SiO_2	Rb	Sr	$(^{87}Sr/^{86}Sr)_m$	$(^{87}Sr/^{86}Sr)_i$	Nd	Sm	$(^{143}Nd/^{144}Nd)_m$	ε_{Nd}
Teniente Mafic Complex (CMET; 8·9 ± 1·4 Ma)									
Ex2004-04	51·9	26	468	0·704070 ± 09	0·70405	16·6	4·00	0·512782 ± 09	+2·9
1411-1630A	50·1	71	472	0·703992 ± 08	0·70396	14·3	3·50	0·512818 ± 07	+3·5
540-2082	51·3	54	535	0·704054 ± 11	0·70404	13·3	3·30	0·512813 ± 11	+3·4
QT-4	49·7	29	595	0·704286 ± 14	0·70421	15·8	3·90	0·512798 ± 09	+3·1
AS-99-1c	57·8	73	547	0·704032 ± 16	0·70402	18·9	3·80	0·512803 ± 06	+3·2
Cerro Montura andesite sills (8·2 ± 0·5 and 6·6 ± 0·4 Ma)									
TTc9	61·0	82	543	0·70396 ± 08	0·70391	25·0	5·13	0·51273 ± 16	+2·7
TTc10	61·5	74	700	0·70390 ± 07	0·70385	21·9	4·26	0·51279 ± 12	+3·0
Sewell Tonalite (7·05 ± 0·14 Ma)									
TTc5	63·7	96	699	0·703930 ± 07	0·70386	19·2	3·39	0·512770 ± 04	+2·7
400S/1780E	62·1	60	946	0·704010 ± 12	0·70404	16·2	2·90	0·512759 ± 36	+2·5
Northern and Central Dacitic Porphyries (6·09 ± 18 Ma)									
2370-159	64·0	124	392	0·704095 ± 12	0·70409	8·3	1·44	0·512802 ± 12	+3·2
1824-655	62·9	142	415	0·704089 ± 12	0·70408	7·4	1·00	0·512767 ± 08	+2·7
Porphyry A (5·67 ± 0·19 Ma)									
1473-970	48·5	209	499	0·704105 ± 10	0·70409	13·4	3·44	0·512799 ± 07	+3·1
1446-266	56·3	187	456	0·704104 ± 12	0·70406	26·1	4·63	0·512795 ± 09	+3·1
Teniente Dacite Porphyry (PDT; 5·28 ± 0·10 Ma)									
1134-302	64·4	65	755	0·704072 ± 12	0·70406	14·4	2·39	0·512757 ± 14	+2·5
1300-403	66·3	67	699	0·704027 ± 12	0·70402	9·0	1·58	0·512762 ± 27	+2·6
1134-79	59·9	87	680	0·704047 ± 13	0·70404	14·1	2·80	0·512785 ± 15	+2·9
Latite dike (4·82 ± 0·09 Ma)									
1394-92	60·9	81	704	0·704051 ± 07	0·70405	15·3	2·70	0·512757 ± 12	+2·5

within the El Teniente deposit do not show these same temporal isotopic variations and all of them are isotopically similar to the Teniente Volcanic and Plutonic Complex rocks, and distinct from the Young Plutonic Complex granitoids.

Teniente Mafic Complex (CMET; 8·9 ± 1·4 Ma)

The oldest rocks within the El Teniente mine are dark colored, with an aphanitic to porphyritic appearance. For many years they were locally known as the 'Andesites of the Mine', but currently they are mapped as the Teniente Mafic Complex (Fig. 3; Skewes & Arévalo, 2000; Burgos, 2002; Skewes *et al.*, 2002, 2005). These rocks are generally strongly altered, brecciated and mineralized, and aspects of their original petrology have been obscured. The name 'Andesites of the Mine' suggests intermediate extrusive rocks, and they have been correlated in the past with the andesitic extrusive rocks of the Farellones Formation (Howell & Molloy, 1960; Camus, 1975; Cuadra, 1986). However, chemical analyses for samples from within the mine indicate SiO_2 contents that range only from 46·5 to 52 wt % (Table 2 and Table 2ES in the Electronic Supplement). This indicates that these rocks are essentially basaltic in composition, although some sills on the extreme margins of this complex, outside the area of the mine itself, are basaltic andesites and andesites, with SiO_2 in the range 56–59·8 wt % (Table 2 and Table 3ES in the Electronic Supplement).

Geological mapping (Fig. 2; Morel & Spröhnle, 1992) indicates that the 'Andesites of the Mine' constitute part of a mafic intrusive complex, with the form of a laccolith, that intruded rocks of the Teniente Volcanic Complex, as was originally suggested by Lindgren & Bastin (1922). The central part of this mafic complex, within which the mine is located, has a vertical extent of >2000 m. The entire complex has a volume of at least 50 km^3, based on an

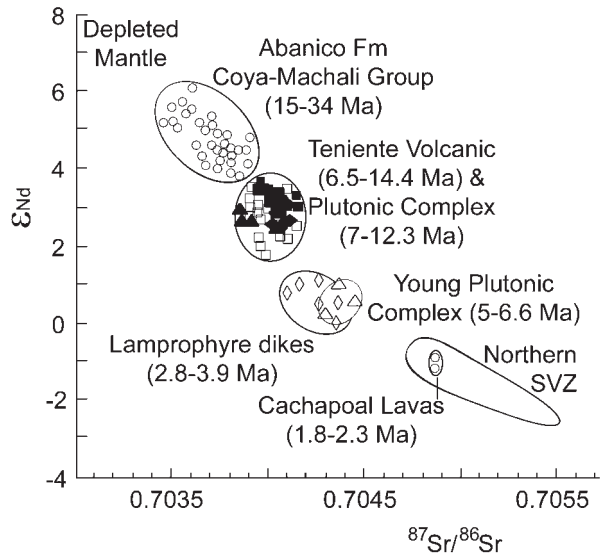

Fig. 5. Published (open symbols) values of $^{87}Sr/^{86}Sr$ vs ε_{Nd} for igneous rocks of different ages from a transect across the Andes at the latitude of El Teniente (34°S), compared with values for samples of the host rocks of the deposit (filled symbols; Table 4), including the Teniente Mafic Complex (■), Sewell Tonalite (▲), felsic porphyries (◆), and Porphyry A granitoid (●). Previously published data are from Stern & Skewes (1995), Kurtz *et al.* (1997), Nystrom *et al.* (2003), Kay *et al.* (2005), Muñoz *et al.* (2006) and Stern *et al.* (2010). Although the youngest felsic plutons in the deposit are the same age (6·09 ± 0·18 to 4·58 ± 0·10 Ma) as rocks from the regionally defined Younger Plutonic Complex (6·6 to ~5 Ma; Kay *et al.*, 2005) they are isotopically similar to the older host-rocks of the deposit as well as to Teniente Volcanic and Plutonic Complex rocks.

estimated overall average thickness of ~1 km. An age of 8·9 ± 2·4 Ma was obtained by fission-track dating on apatite from a mafic sill outside the mine (Maksaev *et al.*, 2004), and a similar age of 8·9 ± 1·4 Ma (Fig. 4) was determined by K–Ar whole-rock analysis of a fresh olivine-bearing sample from the western margin of the mafic complex (sample Ex2004-04).

There is no chemical distinction between the gabbros (Fig. 7a), diabases and basaltic porphyries (Fig. 7b) that form this complex. The least altered samples from within the mine have SiO_2 contents that range between 47 and 52 wt % (Table 2 and Table 2ES in the Electronic Supplement), and chemically they correspond to basalts. They have 6·6–11 wt % CaO and 17–21·5 wt % Al_2O_3, consistent with their high calcic plagioclase content. The FeO content (8–11·6 wt %) is high with respect to MgO (<5·2 wt %), but TiO_2 and P_2O_5 contents are relatively low, consistent with calc-alkaline affinities for these mafic rocks. Their alkali components and volatile contents vary according to the type and degree of alteration. The freshest rocks, from outside the deposit (samples EX2004-04 and AM2; Table 2 and Table 3ES in the Electronic Supplement), have the lowest K_2O (0·5–1·0 wt %; Fig. 8) and H_2O (typically <1·0 wt %). The samples with more intense biotite alteration have higher K_2O and H_2O contents, the latter as high as 3·5 wt % (Fig. 8). However, it is clear that their SiO_2 contents have not been significantly changed by alteration, as the small range of silica contents for samples from within the mine is independent of LOI

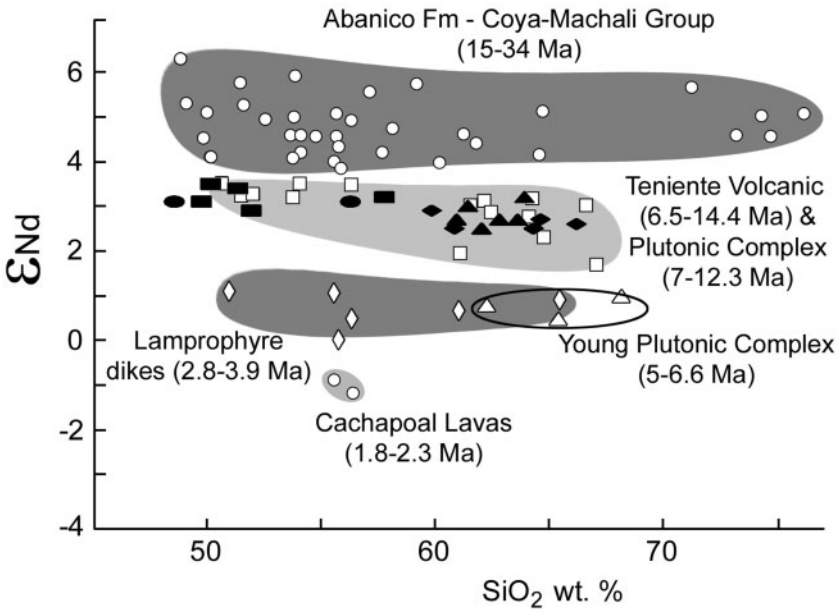

Fig. 6. Published (open symbols; data from same sources as for Fig. 5) values of ε_{Nd} vs SiO_2 (wt %) for igneous rocks of different ages from the transect across the Andes at the latitude of El Teniente (34°S), compared with values for samples of the host-rocks in the deposit (filled symbols as in Fig. 5).

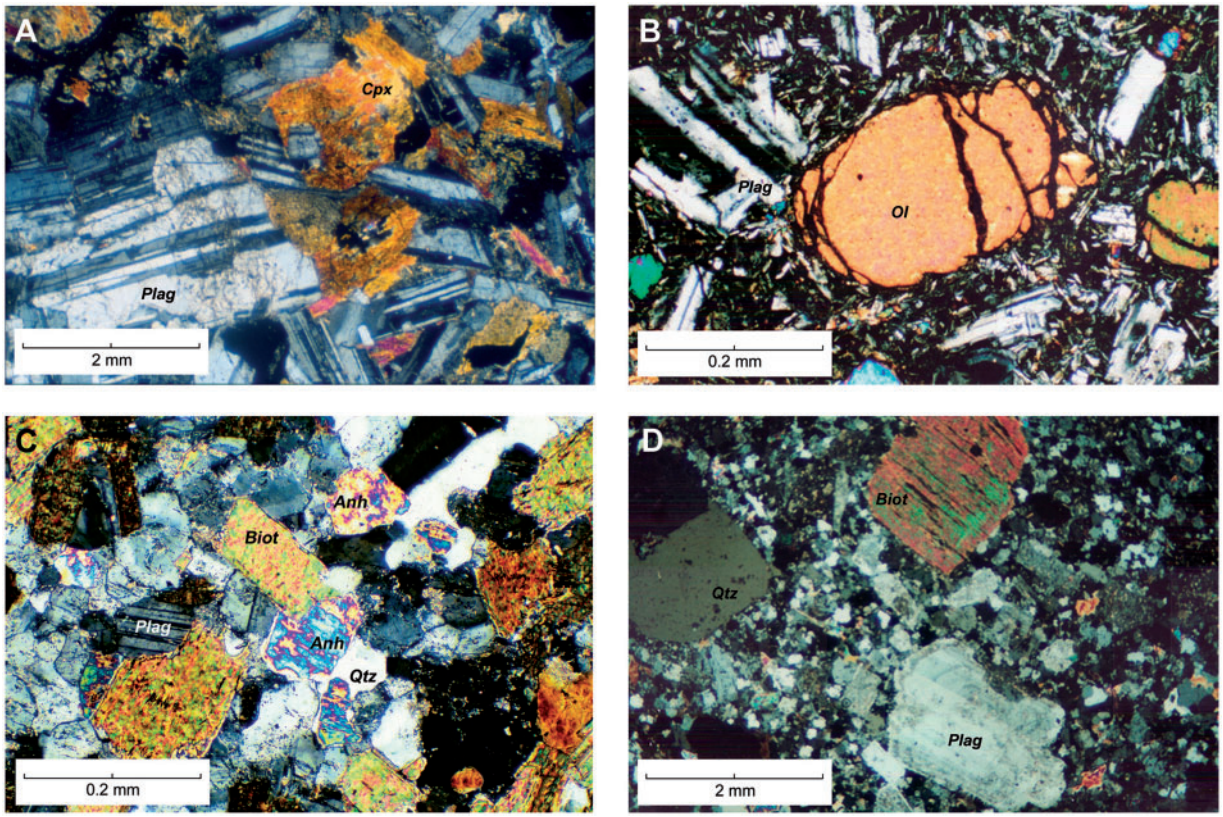

Fig. 7. (a, b) Photomicrographs of two samples from the Teniente Mafic Complex: (a) weakly altered gabbro from within the mine (sample DDH1411-1630'; Tables 1 and 2), containing fresh unzoned calcic plagioclase and Fe–Ti oxides, and secondary actinolite and biotite pseudomorphically replacing olivine (upper left) and clinopyroxene (center); (b) a fresh porphyritic olivine basalt from the margin of the complex, outside the mine (sample EX2004-04; Tables 1 and 2), containing olivine (Fo74; center) and unzoned plagioclase phenocrysts in a finer-grained groundmass of intergrown clinopyroxene, plagioclase and Fe–Ti oxides. (c). Biotite-rich 'andesite' igneous breccia sample DDH1473-940 (Tables 1 and 3), with interstitial anhydrite. It should be noted that the rock is not porphyritic, and in this fresh and unaltered igneous rock neither biotite nor plagioclase are altered to chlorite or sericite. (d) Photomicrograph of PDT sample DDH1134-365' (Table 1ES) with oscillatory zoned plagioclase, rounded quartz 'eyes', and fresh biotite (biot) phenocrysts in a groundmass containing quartz, plagioclase, potassium feldspar, biotite, anhydrite and opaque minerals.

and K_2O (Table 2 and Table 2ES). Also, plagioclase phenocrysts, even in the most strongly altered samples, have not been strongly affected by this alteration and preserve high An contents indicative of mafic rocks. The rocks of the Teniente Mafic Complex were clearly not originally andesites converted into more basic compositions by secondary hydrothermal alteration processes.

The basaltic rocks of the CMET have La/Yb ranging from 3·5 to 8·5 (Figs 9 and 10), Dy/Yb ranging from 1·9 to 2·2 (Fig. 10) and Sr/Y from 19 to 37, and in these respects they resemble the basalts of the Teniente Volcanic Complex. Basaltic andesite and andesite sills outside the mine have higher La/Yb (10–13·7) and Sr/Y (30–39) than the more mafic samples, but similar Dy/Yb (1·9–2·3) to them. Initial $^{87}Sr/^{86}Sr$ ratios of all the samples range from 0·70396 to 0·70421, and ε_{Nd} ranges from +2·9 to + 3·5, values that overlap those of Teniente Volcanic Complex rocks (Figs 5 and 6).

Sewell Tonalite (7·05 ± 0·14 Ma) and associated andesitic sills (8·2 ± 0·5 to 6·6 ± 0·4 Ma)

The Sewell Tonalite is one among a number of intermediate to felsic plutons within the Teniente Plutonic Complex that regionally intruded the Teniente Volcanic Complex rocks between 12·4 and 7·0 Ma (Cuadra, 1986; Kurtz *et al.*, 1997). The equigranular holocrystalline Sewell Tonalite complex crops out over an area approximately half as large as the Teniente Mafic Complex (Fig. 2), with an estimated volume of ~30 km^3 based on an approximate average thickness of ~1 km.

Cuadra (1986) determined two K–Ar ages of 7·4 ± 1·5 and 7·1 ± 1·0 Ma for the tonalite. These two ages are in the range of both a K–Ar age of 7·0 ± 0·4 Ma that he also obtained for the La Huifa pluton, a porphyritic phase of the Sewell Tonalite complex which crops out 2 km NE of the deposit (Fig. 2; Reich, 2001), and $^{40}Ar/^{39}Ar$ step heating

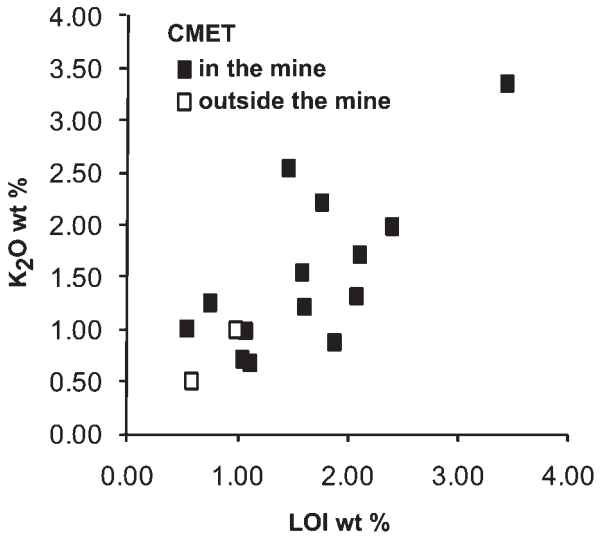

Fig. 8. K_2O vs volatile (LOI, loss on ignition) content (in wt %), of Teniente Mafic Complex samples from within the mine (■; Table 2 and Table 2ES) compared with the freshest samples from outside the mine (□; samples EX2004-04 and AM2; Table 2 and Table 3ES), illustrating the correlation of increasing K_2O and LOI as the intensity of alteration increases. The least altered samples have K_2O <1 wt %. All these samples have SiO_2 between 46·7 and 52 wt %, MgO between 3·5 and 5·8 wt % and FeO >8% (Table 2 and Table 2ES), and they all preserve unaltered calcic plagioclase, indicating that they were originally all basalts, not andesites.

ages (a plateau age of 6·97 ± 0·1 Ma and a total gas age of 7·05 ± 0·14 Ma) determined by Maksaev *et al.* (2004) for this same pluton. Maksaev *et al.* (2004) also determined a younger U–Pb zircon age of 6·15 ± 0·08 Ma for a sample (TT-101) they identified as the Sewell Tonalite, but we do not consider this sample as representative of this pluton (Skewes & Stern, 2007), and this age is younger than a Re–Os age of 6·31 ± 0·03 Ma on molybdenite from a breccias complex intruding the tonalite. Therefore, we consider the total gas age they obtained for the La Huifa pluton to be the best age also for the Sewell Tonalite complex (Fig. 4). Cuadra (1986) also dated andesitic sills at Cerro Montura, a few kilometers NW of the mine, at 8·2 ± 0·5 and 6·6 ± 0·4 Ma (Fig. 4).

The Sewell Tonalite and andesitic sills range in composition from 61 to 66 wt % SiO_2, with 1·5–2·7 wt % K_2O. The La/Yb ratios of the andesitic sills (9·4–13·1) are lower and less variable than those of the tonalite (15·6–44·5; Table 2 and Table 4ES). The tonalite has higher La/Yb (Fig. 9) and Sr/Y, lower Yb and Y, and similar to somewhat higher Dy/Yb (Fig. 10) compared with the mafic rocks of the CMET. $^{87}Sr/^{86}Sr$ ratios (0·70385–0·70410) and ε_{Nd} (+2·2 to + 3·2) are similar for both sills and the tonalite, and overlap with the values for the samples from both the Teniente Volcanic and Teniente Mafic Complex (Figs 5 and 6). Kurtz *et al.* (1997) also reported similar La/Yb

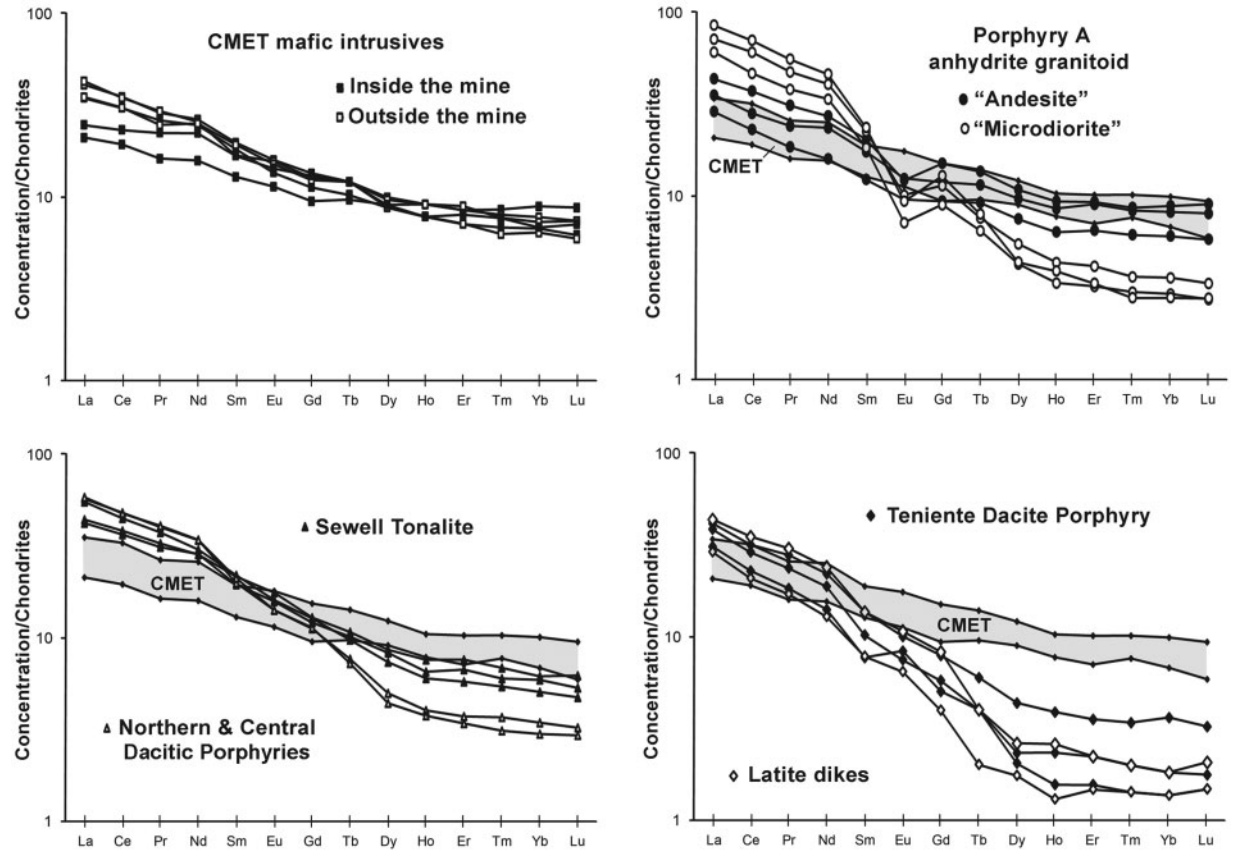

Fig. 9. Rare earth element (REE) concentrations, normalized to chondritic meteorite abundances, for the plutonic host-rocks of the Teniente deposit.

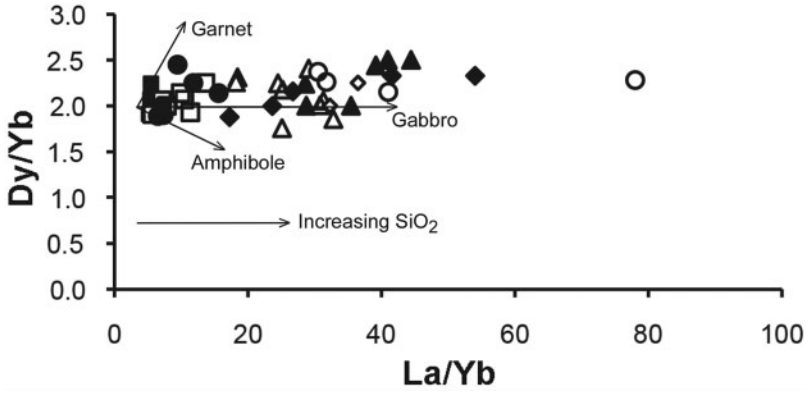

Fig. 10. La/Yb vs Dy/Yb for the host plutons of the Teniente deposit. Symbols are as in Fig. 9. Trends produced by garnet, amphibole and gabbro (clinopyroxene and plagioclase) crystal fractionation are from Davidson *et al.* (2007). SiO_2 content increases towards higher La/Yb.

ratios (9·9–20·9), initial $^{87}Sr/^{86}Sr$ (0·70398–0·70416) and ε_{Nd} (+1·6 to + 2·8) for regionally contemporaneous felsic plutons of the Teniente Plutonic Complex (Kurtz *et al.*, 1997).

Northern and Central dacitic porphyries (6·09 ± 0·18 Ma)

Within the Teniente mine, two small (<1 km^3) dacitic porphyry bodies, the Northern (1000N, 1000E; Fig 3) and Central (700N, 1200E) dacitic porphryies, occur east and NE of the Braden breccia (Fig. 3). Maksaev *et al.* (2004) obtained a U–Pb age of 6·11 ±0·13 Ma for 11 zircons from the Northern dacitic porphyry (sample TT-102), and a very similar overall average age of 6·08 ± 0·22 Ma for 20 zircons from the Central dacitic porphyry (sample TT-90). We consider the total average 6·09 ± 0·18 Ma to be the age of these intrusions (Skewes & Stern, 2007). Based on their age, they would be considered by Kay *et al.* (2005) as part of the regionally defined Younger Plutonic Complex rocks.

The Northern and Central dacitic porphyries have SiO_2 contents between 56·8 and 66·2 wt % and K_2O between 1·9 and 7·1 wt % (Table 3 and Table 5ES). Their La/Yb (18·2–44·3; Fig. 9) and Sr/Y (72–140) ratios are higher than those of the mafic and intermediate rocks of the CMET, but similar to those of the Sewell Tonalite, whereas their Dy/Yb values (1·9–2·3; Fig. 10) are similar to those of both CMET and tonalite samples. Significantly, $^{87}Sr/^{86}Sr$ ratios (0·70408–0·70409) and ε_{Nd} (+2·7 to + 3·2) are similar for both porphyries, as well as being within the range of the Teniente Mafic Complex and Sewell Tonalite samples, and the Teniente Volcanic and Plutonic Complex rocks (Figs 5 and 6). However, they are isotopically unlike Younger Plutonic Complex rocks of similar age and composition, which have higher $^{87}Sr/^{86}Sr$ ratios and lower ε_{Nd}.

Porphyry A anhydrite-bearing stock (5·67 ± 0·19 Ma)

The small (<1 km^3) Porphyry A anhydrite-bearing granitoid stock, which is ~150 m wide at level Teniente-5 (Fig. 3), consists of a number of different lithological units described by Stern *et al.* (2007). The stock intrudes a Cu-rich (>1–2 wt % Cu) magmatic–hydrothermal anhydrite breccia emplaced along the contact between the intrusive rocks of the El Teniente Mafic Complex and the Sewell Tonalite pluton. The margins of the stock are characterized by matrix-supported igneous breccias containing abundant angular and rounded clasts of the surrounding mafic and tonalitic rocks. The matrices of these breccias contain igneous biotite, plagioclase and potassium feldspar, quartz and both primary magmatic and magmatic–hydrothermal anhydrite (Fig. 7c). The igneous breccias have been mapped by mine geologists as 'microdiorite' and 'andesite' breccia depending on the color of their matrix, which ranges from light to dark as the relative proportion of biotite increases. The light-colored Porphyry A 'microdiorite' forming the central clast-free core of the stock, which is volumetrically the dominant rock type, is petrologically equivalent to the matrix of the 'microdiorite' igneous breccias found along its margins.

As noted by Stern *et al.* (2007), the 'andesite' breccia is not extrusive and is not an andesite (Table 3 and Table 6ES), the 'microdiorite' breccia is not a diorite, and none of the rocks that form the Porphyry A stock are porphyritic. These field names are correct only in so far as they suggest that these are igneous rocks. However, they are clearly not typical igneous rocks, and we do not think that any common igneous rock names are appropriate for these unusual rocks, because of the large amount of modal primary igneous anhydrite, sulfur and volatiles (Table 3) they contain, but we do not offer alternative names for these rocks here.

Clast-rich 'microdiorite' igneous breccias from along the margin of the Porphyry A stock have an age determined by U–Pb in zircons of 6·27 ± 0·19 Ma considering all analyzed spots (sample TT-150; Maksaev *et al.*, 2004). However, a bimodal distribution of ages is apparent, with a peak of 6·46 ± 0·11 Ma for 13 zircons and 5·67 ± 0·19 Ma for four zircons. We consider the older peak to represent the average of the multi-lithic clasts in the breccia, and the younger to represent the age of the breccia matrix (Fig. 4; Maksaev *et al.*, 2004; Skewes & Stern, 2007; Stern *et al.*, 2007). Molybdenite in the Cu-rich hydrothermal anhydrite breccia intruded by this stock has been dated by Re–Os at 5·89 ± 0·02 Ma (Cannell *et al.*, 2005) and 5·60 ± 0·02 Ma (Maksaev *et al.*, 2004). These ages are in agreement with the younger U–Pb age in zircons, and they indicate that the formation of this breccia is temporally and therefore genetically related to the intrusion of the Porphyry A stock (Fig. 4).

The anhydrite-bearing plutonic rocks of the Porphyry A stock contain >3 wt % S and >0·5 wt % Cu (Table 3 and Table 6ES). The amount of volatiles lost on ignition (LOI) ranges from 3·1–6·6 wt % for 'andesite' igneous breccias to 8·0–10·4 wt % for Porphyry A 'microdiorite'. However, an indeterminate amount of this LOI is due to the vaporization of sulfur during the ignition process. When normalized for their high LOI and S contents, 'andesite' igneous breccias have major-element compositions comparable with those of basalt (normalized SiO_2 from 49·5 to 52·3 wt %), whereas the Porphyry A 'microdiorite' has compositions similar to andesite (normalized SiO_2 from 56·0 to 61·8 wt %), but with anomalously high CaO that reflects the high modal abundance of anhydrite. Despite their high CaO, the anorthite content of the primary igneous plagioclase in these rocks, which are of basaltic and andesitic composition, is relatively low (An <32).

La/Yb ratios for the 'andesite' igneous breccia range from 6·6 to 15·7, overlapping the range of Teniente Mafic Complex samples and consistent with the mafic composition of these samples (Fig. 9). La/Yb ratios for the 'microdiorite' breccia are higher (30·5–79·9), as a result of both the higher La and lower Yb contents in these samples. The Sr and Nd isotopic compositions of both the 'andesite' and 'microdiorite' igneous rocks are identical to each other (Figs 5 and 6), and they are isotopically similar to all other Late Miocene igneous rocks in the El Teniente deposit, as well as the Teniente Volcanic and Plutonic Complex rocks. However, as with the Northern and Central Dacitic Porphyries, they are isotopically distinct from the contemporaneous felsic granitoids of the Younger Plutonic Complex, which have higher $^{87}Sr/^{86}Sr$ ratios and lower ε_{Nd} (Figs 5 and 6; Kay *et al.*, 2005).

Teniente Dacite Porphyry (5·28 ± 0·10 Ma)

The Teniente Dacite Porphyry is an elongated subvertical dike-like body, extending 1·5 km to the north of the Braden Pipe, with a maximum width of 300 m (Fig. 3). It is truncated to the south by the Braden Pipe, and it is not clear if this porphyry also occurs south of the pipe. Maksaev *et al.* (2004) obtained an age of 5·28 ± 0·10 Ma for zircons from the Teniente Dacite Porphyry dike, which has frequently been cited as the causative igneous intrusion for the mineralization in the deposit (Howell & Molloy, 1960; Camus, 1975; Cuadra, 1986), although it clearly cuts copper mineralized mafic rocks, veins and breccias in the deposit (Skewes *et al.*, 2002, 2005), and its northernmost extension, north of the Teniente River valley (Fig. 2), is unmineralized.

Teniente Dacite Porphry samples have SiO_2 contents from 59·9 to 66·3 wt % and K_2O from 2·6 to 2·9 wt % (Table 3 and Table 5ES). Their La/Yb ratios range from 17·3 to 54·1 (Fig. 9). Sr and Nd isotopic ratios are within the range of all the Late Miocene igneous rocks in the deposit (Figs 5 and 6), and similar to the Teniente Volcanic and Plutonic Complex rocks, but distinct from the contemporaneous felsic granitoids of the Younger Plutonic Complex, which have higher $^{87}Sr/^{86}Sr$ ratios and lower ε_{Nd}.

Latite dikes (4·82 ± 0·09 Ma)

Latite porphyry ring-dikes, 6–8 m wide, occur concentrically surrounding the Braden Pipe (Fig. 3). A small latite porphyry stock is truncated by the Braden Pipe along its northeastern edge (González, 2006). Maksaev *et al.* (2004) obtained a U–Pb age of 4·82 ± 0·09 Ma for zircons from one latite dike (Fig. 5), which is within the range of the age they also determined for the Braden Pipe (4·81 ± 0·12 Ma). The occurrence of blocks of this rock type in the Braden Pipe suggests that that at least some latite porphyry intruded prior to the formation of this breccia pipe, and may have played a role in the formation of the pipe (Floody, 2000; Cannell *et al.*, 2005). Maksaev *et al.* (2004) also obtained a $^{40}Ar/^{39}Ar$ plateau age of 4·58 ± 0·10 Ma for biotite from a small, weakly mineralized dacite intrusion deep in the Braden breccia pipe.

Available chemical analyses indicate that the latite is chemically similar to the Teniente Dacite Porphyry, with 60·9–63·1 wt % SiO_2 and 2·2–3·5 wt % K_2O (Table 3 and Table 5ES), and a high La/Yb of about 35 (Fig. 9). Their Sr and Nd isotopic ratios are similar to those of the Teniente Dacite Porphyry and within the range of all the Late Miocene igneous rocks in the deposit (Figs 5 and 6), and similar to both the Teniente Volcanic and Plutonic Complex rocks, but distinct from contemporaneous felsic granitoids of the Younger Plutonic Complex, which have higher $^{87}Sr/^{86}Sr$ ratios and lower ε_{Nd}.

Post-mineralization lamprophyre dikes (3·85 ± 0·18 to 2·9 ± 0·60 Ma)

The youngest igneous rocks in the deposit are post-mineralization olivine-hornblende-lamprophyre dikes,

dated at 3·85 ± 0·18 to 2·9 ± 0·60 Ma (Cuadra, 1986; Maksaev *et al.*, 2004). These mafic, dark green to black in color, fresh or only weakly altered, post-mineralization, sub-vertical dikes occur both within the El Teniente mine and in the vicinity of the mine (Cuadra, 1986; Stern *et al.*, 2010).

The lamprophyre samples with olivine have SiO_2 contents of 51–53 wt %, Ni of 70–190 ppm and Cr 280–390 ppm. Olivine-free lamprophyres range in composition from 55 to 67 wt % SiO_2 and have lower Ni (<100 ppm) and Cr (<200 ppm) than the more mafic olivine-bearing lamprophyres. The lamprophyre dikes have relatively high Sr (642–916 ppm), low Y (12–17 ppm) and consequently high Sr/Yb ratios (43–71), similar to adakitic andesites; however, these rocks, which range from basaltic to dacitic in composition, are not adakites (Stern *et al.*, 2010). The more mafic lamprophyre samples have low La/Yb ratios (10–13) that are within the range of mafic rocks in the youngest units of Late Miocene Teniente Volcanic Complex (9·2–13·2; Kay *et al.*, 2005) and plutonic rocks of the Teniente Mafic Complex. However, the other less primitive olivine-free lamprophyre dikes have both lower Yb (0·80–0·93 ppm) and higher La/Yb ratios (18–22) compared with the more mafic lamprophyres (Stern *et al.*, 2010).

The lamprophyre dikes have $^{87}Sr/^{86}Sr$ from 0·70410 to 0·70435 and $\varepsilon_{Nd} = +1{\cdot}1$ to $+0{\cdot}2$ (Figs 5 and 6; Stern & Skewes, 1995; Kay *et al.*, 2005; Stern *et al.*, 2010). These isotopic values are higher and lower, respectively, than those of other Late Miocene plutonic rocks from the El Teniente deposit, but similar to the isotopic compositions of the Younger Plutonic Complex.

DISCUSSION

The Late Miocene and Pliocene plutonic rocks that host the El Teniente deposit formed over a relatively brief ~4·3 Myr period, between 8·9 ± 1·4 and 4·58 ± 0·10 Ma (Fig. 4), during the waning stages of an extended Andean magmatic episode that began in the Oligocene. These plutons, which intruded rocks of the Teniente Volcanic Complex, include initially the relatively large Teniente Mafic Complex laccolith (8·9 ± 1·4 Ma), followed by the intrusion of the somewhat smaller equigranular, holocrystalline Sewell Tonalite (7·05 ± 0·14 Ma). These two plutions overlap in age with the final stages of formation of the Teniente Volcanic Complex (14·4–6·5 Ma), and the ages of other plutons in the regionally defined Teniente Plutonic Complex (12·3–7·0 Ma; Fig. 4). After volcanism in the region ceased, a sequence of much smaller porphyritic felsic stocks and dikes intruded between 6·09 ± 0·18 and 4·58 ± 0·10 Ma, the age of the regionally defined Younger Plutonic Complex (6·6 to ~5 Ma; Fig. 4), into the very restricted 2 km × 3 km area within which the deposit is now mined (Fig. 3).

Kay *et al.* (2005) concluded that the differences in the isotopic composition of the Younger Plutonic Complex rocks (6·6 to ~5 Ma) from older Teniente Volcanic (>6·5 Ma) and Plutonic Complex rocks (>7·0 Ma), as well as the higher La/Yb, Sr/Y and other more 'adakitic' petrochemical characteristics of the Younger Plutonic Complex felsic rocks, imply differences in magma source regions and depths of crustal magma generation or fractionation. They attributed the generation of the more 'adakitic' Younger Plutonic Complex felsic rocks in part to melting of the base of the crust that thickened during the Late Miocene. Kay *et al.* (1999) also suggested, in an earlier paper, but in the context of this same model, that fluids released by the breakdown of hydrous phases in the lower crust as the crust thickens contribute to mineralization processes in the Andes.

Significantly, however, the felsic plutonic rocks within the El Teniente deposit do not show the same isotopic shift to higher $^{87}Sr/^{86}Sr$ ratios and lower ε_{Nd} (Figs 5 and 6) that occurs between the regionally defined Teniente Plutonic Complex (12·3–7·0 Ma) and the Younger Plutonic Complex (6·6 to ~5 Ma). Furthermore, in a recent study of zircons separated from each of the felsic units in the deposit, Muñoz *et al.* (2009) demonstrated that all samples have high initial $^{176}Hf/^{177}Hf$ ratios and positive εHf_i with values ranging from +6·2 to + 8·5, and there are no distinct differences among the analyzed igneous units. They concluded that these characteristics are consistent with a common magmatic system being the source of the different intrusive pulses for which the high εHf_i values record a relatively juvenile mantle source. We agree, and conclude that the plutonic rocks that host the deposit were not derived from progressively deepening crustal sources. Instead, we suggest, as elaborated below, that the small volume of late felsic porphyries with 'adakitic' geochemical characteristics (high La/Yb and Sr/Y) were formed during the final stages of crystallization of a large, long-lived, shallow magma chamber (Fig. 11), and that this magma chamber was also the source of the aqueous fluids that generated the mineralized breccias and veins in the deposit, as well as the metals they carried.

Based on a review of information concerning giant Cu deposits, both Cloos (2001) and Richards (2003, 2005) outlined models for their generation involving large magma chambers from the cupola of which are derived the felsic porphyries, magmatic–hydrothermal mineralizing fluids and metals that form such deposits. For El Teniente, the conclusion that the mineralizing aqueous fluids and metals were derived from the same magmas as formed the host plutons in the deposit is based directly on three lines of evidence. First is the overlap in the timing of their formation (Fig. 4). Alteration and mineralization at El Teniente occurred over essentially the same time period as the emplacement of the felsic host plutons, between at

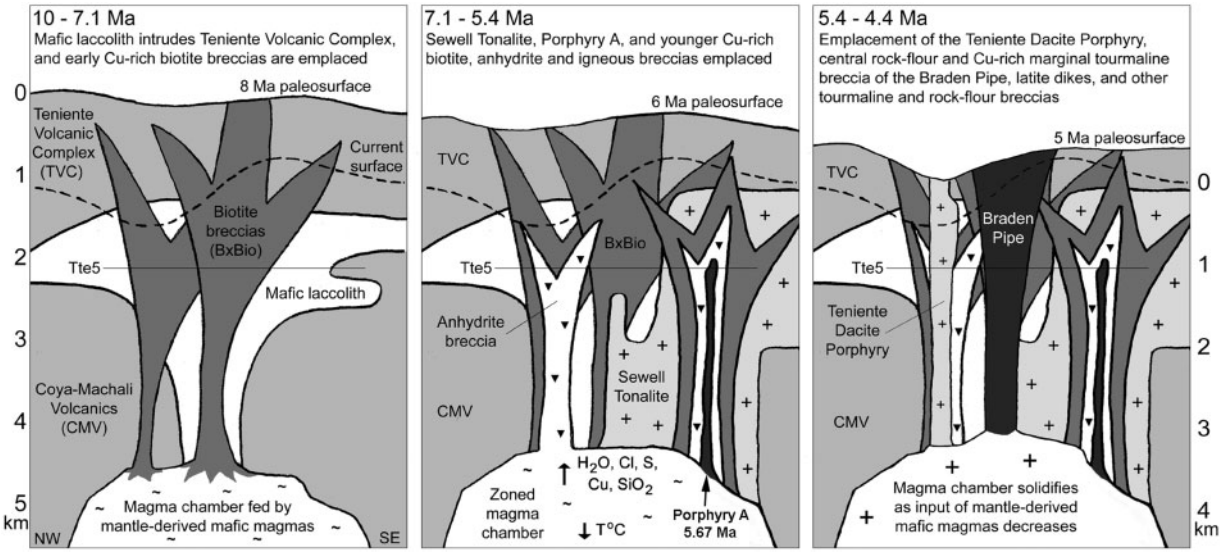

Fig. 11. Model for the multistage development of the El Teniente deposit, modified from Skewes *et al.* (2002) and Stern & Skewes (2005). The main features of the model include (1) a large, long-lived (>2 Myr) open-system magma chamber, crystallizing at >4 km depth, fed from below by mantle-derived mafic magmas and exsolving aqueous fluids through its roof to produce the large breccia pipes that are prominent features in each deposit; (2) decreasing magma supply in the Late Miocene and Pliocene as subduction angle decreases, leading to crystallization and solidification of this chamber; (3) progressive uplift and erosion that enhances this crystallization and solidification process and results in telescoping of different types of breccia and igneous rocks; (4) progressive igneous differentiation of the magma chamber associated with crystallization and volatile loss, generating felsic porphyries that intrude previously mineralized rocks above the chamber. No coeval volcanism is known to have occurred during mineralization, but once the chamber solidified, post-mineralization lamprophyre dikes were emplaced.

least >7·05 ± 0·14 Ma and 4·42 ± 0·02 Ma (Fig. 4; Skewes & Stern, 2007). Although 18 molybdenite Re–Os mineralization ages range from only 6·31 ±0·02 to 4·42 ± 0·02 Ma (Maksaev *et al.*, 2004; Cannell *et al.*, 2005), mapping and petrological studies at El Teniente have shown that at least one widespread event of biotitization and mineralization predates emplacement of the Sewell Tonalite, and that this felsic intrusion cuts biotitized Teniente Mafic Complex rocks and mineralized biotite veins (Skewes & Stern, 2007). This implies that the Re–Os ages for molybdenite obtained in the deposit record only the last 1·9 Myr of mineralization and that the temporal extent of mineralization was actually greater. The lack of older Re–Os ages may reflect the fact that the early widespread mineralization associated with biotitization of the Teniente Mafic Complex generally does not result in the deposition of considerable molybdenite, or coarse molybdenite suitable for dating (Rabbia *et al.*, 2009).

Second, fluid inclusions in quartz-bearing veins at various stages of alteration at El Teniente (Skewes *et al.*, 2002, 2005; Cannell *et al.*, 2005) are consistent with precipitation from highly saline, high-temperature magmatic fluids, both boiling and non-boiling, as well as other fluids with variable salinity, including low-salinity vapor-rich inclusions that may have played an important role in transporting and depositing metals (Klemm *et al.*, 2007). Calculated at temperatures derived from either homogenization temperatures of boiling fluids, or the anhydrite–chalcopyrite sulfur isotope geothermometer (Kusakabe *et al.*, 1984, 1990), the $\delta^{18}O$ of the fluids from which quartz and anhydrite in these veins precipitated was +5·8 to + 6‰, and the δD of fluids that precipitated sericite in vein haloes is −35‰, similar to aqueous fluids derived from cooling magmas (Skewes *et al.*, 2002, 2005). Based on homogenization temperatures (>525°C) for coexisting vapor-rich and highly saline fluid inclusions in quartz from both biotite and tourmaline-rich breccias, Skewes *et al.* (2002, 2005) calculated $\delta^{18}O$ of +6·9 to + 10·6‰ and δD of −36‰ for the boiling aqueous fluid that precipitated this quartz, consistent with exsolution of the breccia-generating fluids from a cooling magma.

Finally, for El Teniente, radiogenic isotopes also imply that the metals in the deposit were derived from the same magmas as those that formed the host-rocks of the deposit. Lead isotope ratios, measured in galena in the deposit ($^{206}Pb/^{204}Pb = 18{\cdot}57$, $^{207}Pb/^{204}Pb = 15{\cdot}60$, and $^{208}Pb/^{204}Pb = 38{\cdot}49$; Puig, 1988; Zentilli *et al.*, 1988), are within the range of the published Pb isotopic compositions of the Late Miocene Teniente Volcanic and Plutonic Complex rocks (Kurtz *et al.*, 1997; Kay *et al.*, 2005), consistent with the derivation of this lead, and by implication the copper in the deposit, from Late Miocene magmas (Stern & Skewes, 2005). Osmium is also derived from the igneous rocks in the deposit, as indicated by the similarity

of $^{187}Os/^{188}Os$ ratios, measured in chalcopyrite, sphalerite and bornite precipitated at different alteration stages during formation of the deposit (Freydier *et al.*, 1997). If these metals had been derived from the surrounding country rocks, greater variability in the $^{187}Os/^{188}Os$ ratios would be expected. These osmium isotopic ratios, which range from 0·171 to 0·223, are more similar to mantle (0·13) than crustal ($\gg$1·0) values, consistent with the derivation of Os and other metals from magmas formed in the sub-Andean mantle, which was also the source for the magmas that formed the host plutons in the deposit. Finally, $\delta^{34}S$ values of sulfides (chalcopyrite and pyrite) from El Teniente range from $-5{\cdot}6$ to $+1{\cdot}6$‰, and average approximately $-2{\cdot}2$‰ (Kusakabe *et al.*, 1984, 1990). This small range is consistent with derivation of sulfur only from igneous rocks associated with the deposit. A calculated total sulfur isotopic composition of $+4{\cdot}5$‰ for El Teniente (Kusakabe *et al.*, 1984, 1990) is also similar to the $\delta^{34}S$ values of non-mineralized Andean granitoids, which range from $+3{\cdot}3$ to $+6{\cdot}1$‰ (Sasaki *et al.*, 1984).

The size, time period of emplacement, and genesis of the different Cu-mineralized breccia pipes and associated veins at El Teniente therefore constrain various aspects of the processes of crystallization and devolatilization in the underlying magma chamber from which the igneous rocks that host the deposit were derived. Most significantly, the amount of Andean magma with 100 ppm Cu required to provide the ~100 Mt of Cu in the deposit would be >600 km^3 if the mechanism of extraction of the Cu is <100% efficient (Stern & Skewes, 2005). This is consistent with the calculation of Cline & Bodnar (1991) of 60 km^3 of magma with 62 ppm Cu to produce the 6 Mt of copper in the Yerington deposit in Nevada, and with the calculations of Cloos (2001) and Richards (2005) that batholith-size volumes of magma (>1000 km^3) are required to generate giant Cu deposits. Compilations of Cu contents for arc andesites (median of 60 ppm; Gill, 1981) and arc rocks with $SiO_2 > 52$ wt % (average of 70 ppm; Stanton, 1994), are lower than 100 ppm, which would imply even more magma required to produce the El Teniente deposit. However, we consider the Cu content of more mafic basaltic magma to be the appropriate value to use, as it was sub-arc mantle-derived basalts that recharged the magma chamber or magmatic plumbing system above which the Teniente deposit formed. A sample of a fresh olivine basalt from the Teniente Mafic Complex (sample Ex2004-04; Table 2), which represents the type of basalt initially emplaced in the area of the deposit, has 115 ppm of Cu. Post-mineralization Pliocene olivine lamprophyres, the type of mafic magma that was forming in the mantle after the deposit formed, have Cu contents that range from 80 to 100 ppm and average 92 ppm (Stern *et al.*, 2010). Therefore we consider a value of 100 ppm appropriate for calculating the amount of mantle-derived magma from which the Cu in the deposit was ultimately derived.

The full volume of magma from which the Cu was extracted may have resided in a single large, long-lived magma chamber, or may represent the integrated volume of multiple smaller magma batches forming independent magma chambers and intrusions at different times during the >2 Myr period of mineralization. For the five reasons listed below, we prefer a model of a single, large, long-lived chamber or magmatic plumbing system during the period when the felsic intrusions that host the deposit and the most prominent dated breccias in the deposit formed.

(1) The lack of occurrence of any mafic rocks in the time period $<8{\cdot}9 \pm 1{\cdot}4$ to $>3{\cdot}85 \pm 0{\cdot}18$ Ma suggests that a single magma chamber, or the integrated magmatic plumbing system, acted as a trap within which mafic mantle-derived magmas were mixed and thus unable to reach the surface.

(2) The isotopic similarity of all the igneous rocks emplaced during this time period (Figs 5 and 6) also suggests a large well-mixed system, particularly in light of the fact that on a regional scale, smaller isolated felsic plutons of the Younger Plutonic Complex (Kay *et al.*, 2005) have different isotopic compositions from the contemporaneous felsic plutons inside the Teniente deposit. This isotopic change is not observed in the felsic plutons within the Teniente deposit, suggesting that a single large, long-lived system acted as a sponge within which small volumes of isotopically distinct melts may have mixed without noticeably changing the isotopic composition of the larger system.

(3) The sequence from initially mafic to progressively smaller volumes of isotopically similar felsic differentiates, which can all be explained by fractionation of olivine, plagioclase, pyroxene, amphibole and accessory phases, is consistent with a single chamber or integrated system progressively cooling and crystallizing as subduction angle, and consequently the supply of mantle-derived magma recharging the system, decreased from the Late Miocene to the Pliocene.

(4) The formation of multiple mineralized breccia pipes and veins contemporaneous with the intrusion of the felsic plutons in the deposit requires the exsolution of large volumes of magmatic volatiles from the roof or cupola of a magma chamber. The quantity of volatiles, sulfur and metals in the deposit requires scavenging from a relatively large volume of magma, which could be provided by the progressive cooling of a single large chamber.

(5) Cannell *et al.* (2005) suggested that vein distributions in the deposit were controlled by a local stress regime generated by the intrusion of a large, 4–6 km deep

magma chamber that they also interpreted as the source of the felsic porphyries, Braden Pipe and Cu in the deposit.

The development of a large batholith-sized magma chamber, containing at least ~600 km^3 of magma, during a >2 Myr period, from $7{\cdot}05 \pm 0{\cdot}14$ to $4{\cdot}58 \pm 0{\cdot}01$ Ma, when compression prevented volcanism, is consistent with known magma extrusion and production rates in the Andes. Stern *et al.* (1984) determined that the 105 km^3 cone of the Maipo volcano, which formed over only the last 450 kyr in the High Andes at the same latitude (34°S) as El Teniente, required extrusion rates of 236 km^3/Myr. If none of this magma had extruded, it could create an ~600 km^3 chamber in ~2 Myr. This rate is at the low end of other estimates of extrusion rates in the Andes (Baker & Francis, 1978; Hildreth *et al.*, 1984), and extrusion rates are certainly lower than total magma production rates. Magma chambers of this size have occurred at this latitude of the Andes, as indicated by the eruption of the 450 km^3 tuff of Pudahuel from the Maipo caldera (Stern *et al.*, 1984), and much larger magma chambers are implied by the volumes of single eruptions of silicic magmas in the Central Andes of northern Chile (de Silva, 1989).

Studies of the time frame in which crystal–melt segregation takes place from crystal mushes (10^4–10^5 years; Bachman & Bergantz, 2004), residence times of silicic magmas in the crust as indicated by Rb/Sr isochrons (7×10^5 years; Halliday *et al.*, 1989), crystal growth rates as implied by spot U–Pb analysis of magmatic zircons (3×10^5 years; Reid *et al.*, 1997; Brown & Fletcher, 1999), $^{238}U/^{230}Th$ ratios in rhyolites constraining differentiation time scales (>10^5 years; Hawkesworth *et al.*, 2000), and time scales estimated to build batholith-size plutons and allow them to cool (10^5–10^6 years; Koyaguchi & Kaneko, 1999; Jellinek & DePaolo, 2003) approach the lifetime of the processes of felsic pluton intrusion and mineralized breccia emplacement at Teniente. Maksaev *et al.* (2004) reported bimodal zircon age populations ($6{\cdot}46 \pm 0{\cdot}11$ and $5{\cdot}67 \pm 0{\cdot}19$ Ma) from different spot U–Pb ages on single zircons from the Porphyry A 'microdiorite' and suggested that the older group of ages may indicate zircons inherited from a crystallizing magma chamber. Cannell *et al.* (2005) interpreted changes in vein orientation in the deposit to reflect various stages of subsidence and resurgence of the magma chamber underlying the Teniente deposit. We therefore suggest that the episodic recharge of the magma system below Teniente by hot mantle-derived mafic magma could either maintain the system as a single chamber for a protracted period, or reheat and reactive the system through a series of thermal oscillations that allow felsic melts to form, and large quantities of volatiles, sulfur and metals to concentrate near the top of the system episodically over an extended period of time.

Another important implication of the suggestion that the mineralized breccia pipes, veins and Cu ore in the deposit were derived from the same magmatic plumbing system as the igneous rocks concerns the depth to the top of this system. This must have been below the roots of the breccia pipes, or >4 km based on the fact that these roots occur at >1 km below the deepest level of mining and exploration drilling, which is >3 km below the current surface and deeper below the paleosurface. Cloos (2001) and Richards (2003, 2005) suggested that large magma chambers below giant Cu deposits are disk shaped and that they focus felsic intrusions and volatile exsolution through a narrow cupola. This is consistent with the observation at Teniente that the ~100 Mt of Cu in the deposit is concentrated into a very small 6 km^2 area (Fig. 3) of brecciated and altered host-rocks into which the youngest felsic porphyries intruded. Cloos (2001) suggested that disk-shaped magma chambers of this size may form at the density discontinuity between crystalline basement and the sedimentary cover, at depths of 6–15 km. Below Teniente an upper crustal density discontinuity probably occurs at the contact between the Coya-Machalí volcanic rocks and the older crystalline basement. Together the Teniente Volcanic Complex and Coya-Machali volcanic rocks are ~6 km thick, and we suggest that this is where the initial magma chamber below the Teniente deposit may have formed (Fig. 11). With time, uplift and erosion brought the roof of the chamber closer to the surface, but never closer than 4 km, which is the minimum estimate of the depth of the roots of the larger mineralized breccias in the deposit. Also, as discussed in detail by both Cloos (2001) and Richards (2003, 2005), shallower chambers (<4 km) may lose volatiles without concentrating metals, as the solubility of Cl and metals is lower in aqueous-rich fluids at low pressure. Deeper, mid- to lower crustal chambers may also underlie and supply magmas to the relatively shallow chamber below the site of formation of a large Cu deposit (Cloos, 2001; Richards, 2003, 2005; Annnen *et al.*, 2006), but the thermal gradients in deeper chambers may not be as high as in a shallower chamber, inhibiting volatile transfer and concentration of volatiles at the top of the chamber. Furthermore, deeper chambers may never reach volatile saturation; a relatively shallow (4–6 km depth) cupola is implied for El Teniente by the multiple events of magmatic volatile exsolution and mineralized breccia emplacement that generated the deposit (Skewes *et al.*, 2002, 2005).

Magmatic differentiation processes taking place in a large magma chamber include a complex combination of recharge of the base of the chamber by mantle-derived mafic magmas, thermal stratification and convection, magma mixing and crystallization, bubble formation, and volatile transfer and concentration in the upper cooler parts of the chamber, as outlined for such large chambers in general by Shinohara *et al.* (1995), Cloos (2001), Hattori

& Keith (2001), Richards (2003, 2005) and Heinrich *et al.* (2005). The petrochemistry of the sequence of plutons within El Teniente constrains some aspects of the timing of development and evolution of the magma chamber below this deposit.

Teniente Mafic Complex (8·9 ± 1·4 Ma)

The oldest pluton in the deposit, the Teniente Mafic Complex (CMET), is a laccolith formed by mafic magmas. These magmas petrochemically resemble contemporaneous mafic volcanic rocks of the youngest unit, the Upper Sewell Group (9·3–6·5 Ma), of the Teniente Volcanic Complex. Because the basalts in the core of the Teniente Mafic Complex, inside the mine, resemble the most mafic members of the Upper Sewell Group, they may have come directly from the sub-arc mantle, without significant fractionation or residence time in any upper crustal magma chamber. We conclude that the large upper crustal magma chamber that subsequently formed below the area of the Teniente deposit (Fig. 11) did not exist at the time of the emplacement of the CMET.

Sewell Tonalite and andesite sills (8·2 ± 0·5 to 6·6 ± 0·4 Ma)

The Sewell Tonalite and sub-contemporaneous andesite sills are intermediate in composition and both contain amphibole crystals. Chemically these rocks resemble intermediate plutons of the Teniente Plutonic Complex. As discussed by Kay *et al.* (2005), their chemistry may be explained by derivation from more mafic, but isotopically similar, Teniente Volcanic Complex magmas by crystal fractionation involving amphibole along with pyroxene, plagioclase and accessory phases. In the case of the Sewell Tonalite, this model is consistent with the higher La/Yb and SiO_2, but similar Dy/Yb (Fig. 10) of this tonalite compared with the isotopically similar basaltic rocks of the Teniente Mafic Complex.

The process of fractionation required to produce this relatively large tonalite pluton implies at least a moderate-sized upper crustal magma chamber from which both porphyritic felsic rocks, such as those that occur at La Huifa (Reich, 2001), and the larger equigranular phases of this pluton can form. This pluton was generated when volcanism was still active, and zoning in plagioclase crystals in the tonalite suggests fluctuating water pressure at relatively shallow conditions. We suggests that the Sewell Tonalite formed during the early developmental and progressive growth phase of the magma chamber that subsequently evolved into the larger chamber that generated both the dated mineralized breccias and felsic porphyries in the deposit between 6·31 ± 0·03 and 4·42 ± 0·02 Ma (Fig. 4). However, the Sewell Tonalite cuts early mineralized veins in the Teniente Mafic Complex (Skewes & Stern, 2007), indicating that the earliest stages of mineralization in the deposit reflect processes of devolatilization of this moderate-sized chamber prior to the intrusion of the tonalite (Fig. 11).

Felsic porphyries (6·09 ± 0·18 to 4·58 ± 0·10 Ma)

The Northern and Central Dacitic Porphyries, Teniente Dacite Porphyry and latite dikes all have features in common. They were intruded after volcanism in the area stopped, and their age corresponds to the terminal stages of the regionally defined Young Plutonic Complex. Both the felsic porphyries within El Teniente and the Young Plutonic Complex rocks have high La/Yb and Sr/Y. Kay *et al.* (2005) attributed these features to equilibration with a high-pressure, plagioclase-poor, garnet-bearing residual mineral assemblage formed in the deep crust as the crust thickened owing to Late Miocene deformation. This may be the case for the Young Plutonic Complex rocks outside the deposit, which have different isotopic compositions from the older Teniente Volcanic and Plutonic Complex rocks, suggesting an isotopically distinct, possibly deeper source. However, the small volume of felsic porphyries inside the Teniente deposit are isotopically similar to both the mafic rocks of the Teniente Mafic Complex and Sewell Tonalite, and we suggest that they were formed by low-pressure fractional crystallization processes near the roof of the large magma chamber that crystallized and solidified under the Teniente deposit between ~6·3 and ~4·4 Ma. As outlined above, the presence of this chamber during this time period is implied by the contemporaneous episode of breccia formation and mineralization (Fig. 4) resulting from exsolution of magmatic fluids that had scavenged large quantities of volatiles, metal and sulfur from a large magma body. Magmas formed at greater pressures, below this chamber, such as mantle-derived magmas or deep-crustal melts similar to those that formed the Young Plutonic Complex rocks, did not reach the surface because they mixed into the magma in this chamber.

That the felsic porphyries in El Teniente equilibrated near the top of a relatively shallow magma chamber is also indicated by their porphyritc texture, large proportion of phenocrysts implying that they intruded as crystal mushes, and the complex oscillatory zoning exhibited by plagioclase crystals that is interpreted to reflect fluctuation of volatile pressure in a shallow crustal environment. Some of the samples of these felsic porphyries contain what appears to be primary igneous anhydrite, a phase produced by saturation with oxidized sulfur, consistent with their formation near the volatile-rich roof of a shallow magmatic system, not in the deep crust.

Amphibole is a common phenocryst in the porphyries, and we suggest that these magmas formed by fractional crystallization in the shallow magma chamber involving amphibole, as well as various processes too complicated for evaluation by simple models of trace-element evolution, such as recharge by mafic magmas, magma mixing, and

volatile diffusion. The felsic porphyries have higher La/Yb and SiO_2 than the basaltic rocks of the Teniente Mafic Complex, but similar Dy/Yb, consistent with fractionation of amphibole, clinopyroxene and plagioclase, but not garnet (Fig. 10; Davidson *et al.*, 2007; Richards & Kerrich, 2007).

Porphyry A (5·67 ± 0·19 Ma)

Despite the abundance of unambiguously hydrothermal anhydrite in this deposit, we argue that anhydrite in the igneous rocks forming the Porphyry A stock, as well as in some of the other felsic porphyries, is either a strictly magmatic or magmatic–hydrothermal phase (Stern *et al.*, 2007). It is clear petrographically that anhydrite and other major minerals in this stock are primary phases that crystallized together in the melt-filled space occupied by the stock, and are not secondary replacement phases of any pre-existing rock. The Porphyry A 'andesites' and 'microdiorites' have REE contents similar to those of Teniente Mafic Complex rocks and the Sewell Tonalite, respectively (Fig. 9), which also suggests that these are igneous rocks and not the product of extreme alteration of pre-exisiting felsic porphyries, all of which have higher La/Yb. The fact that anhydrite crystallized contemporaneously with the other silicate minerals in this stock is suggested by its planar crystal boundaries with these minerals, and the inclusion of silicates in anhydrite and anhydrite in silicates. Furthermore, we suggest that the relatively sodic content of plagioclase in these rocks, which are of basaltic and andesitic composition, is due to the simultaneous crystallization and sequestering of Ca by anhydrite. The similarity of oxygen-isotope temperatures calculated from anhydrite–quartz and anhydrite–magnetite mineral pairs to those calculated from quartz–magnetite is consistent with co-crystallization of these three phases (Stern *et al.*, 2007).

Cross-cutting relations and chronological (Fig. 4) data suggest that the emplacement of the Porphyry A pluton occurred in conjunction with the generation of the Cu-rich anhydrite breccia pipe into which it intrudes. Generation of this anhydrite breccia by the exsolution of Cu- and S-rich magmatic fluids from the parent magma chamber occurred together with, or was followed immediately by, the intrusion of the volatile-saturated and Cu- and S-rich silicate magma from this same chamber that produced the small Porphyry A pluton. In this sense, we consider the Porphyry A stock and surrounding contemporaneous anhydrite breccia it intrudes to be the SO_2-rich equivalent of a carbonatite complex, in which SO_2-rich silicate melts and their associated magmatic fluids were emplaced together to produce a variety of genetically related rocks.

The poikilitic texture of anhydrite in the Porphyry A 'microdiorite' indicates late crystallization and growth of anhydrite relative to the silicate phases in this rock. Stern *et al.* (2007) suggested that this occurred as a result of precipitation of magmatic–hydrothermal anhydrite from the magmatic volatiles escaping the underlying magma chamber along with the Porphyry A magma, and that this process enhanced the CaO, Cu and S contents and resulted in the high LOI of the 'microdiorite' relative to normal igneous rocks. Thus we consider the high modal abundance of magmatic–hydrothermal anhydrite and high CaO, Cu, S and LOI of the Porphyry A 'microdiorite' as a primary feature of its chemistry, resulting from the crystallization of a supersaturated mixture of cogenetic silicate magma plus magmatic fluids derived together from the same underlying magma chamber, and not from a two-stage process of magma crystallization followed by later secondary hydrothermal alteration. The volumetrically less significant 'andesite' igneous breccias contain lower modal proportions of interstitial anhydrite that appears texturally to be strictly magmatic anhydrite, crystallized in a single stage at the same time as the silicate minerals that form these rocks. The volatile contents of the 'andesite' breccias are similar to the compositions expected for volatile-saturated basalts at >1 kbar pressure (LOI = 2–4 wt %).

The Cu- and S-rich magmas that formed the anhydrite-bearing Porphyry A pluton and its marginal igneous breccias were sourced from the same chamber as the other felsic porphyries in the deposit, as indicated by their isotopic similarity to all the other igneous rocks in the deposit (Figs 5 and 6). Therefore, these magmas must have formed by magmatic differentiation processes taking place in this large magma chamber. The more felsic 'microdiorites' have higher La/Yb and lower Yb than the more mafic 'andesites', but similar Dy/Yb to them, consistent with amphibole fractionation (Fig. 10). However, sequestering of Ca from the melt by the crystallization of anhydrite may also be responsible for inhibiting the growth of amphibole in the rocks themselves. Although amphibole is a common phase in other igneous rocks containing magmatic anhydrite (Scaillet & Evans, 1999; Barth & Dorais, 2000), these generally contain <2 modal % anhydrite, and those that are volcanic are not fully crystallized and equilibrated as are the plutonic rocks that form the Porphyry A stock.

The unusual Cu- and S-rich Porphyry A magmas formed during a period of compressive deformation, uplift and erosion (Skewes & Holmgren, 1993; Skewes & Stern, 1994; Kurtz *et al.*, 1997; Garrido *et al.*, 2002), with no evidence of coeval volcanic activity in the area of the deposit (Fig. 4; Skewes *et al.*, 2002, 2005; Kay *et al.*, 2005). Compressive deformation and lack of volcanic activity during the Late Miocene may have prevented devolatilization of the magma in the large, long-lived magma chamber underlying the El Teniente deposit (Pasteris, 1996; Oyarzún *et al.*, 2001; Richards *et al.*, 2001). These conditions

allowed the SO_2 and H_2O contents of magmas near the roof of this chamber to increase to the point that they generated the multiple breccia pipes in the deposit, one of which was subsequently intruded by the Cu- and S-rich magmas that crystallized to form the igneous anhydrite-bearing Porphyry A pluton. We consider volatile transport by bubble formation and resorption (Cloos, 2001) as the physical process responsible for concentration of volatiles within the relatively cool cupola of the magma chamber below the deposit (Fig. 11). The relatively high pressure (>1 kbar) at the roof of the magma chamber underlying the El Teniente deposit at >4 km depth, combined with the Cl-rich nature of the volatile-saturated magma near the roof of this chamber, as evidenced by the high salinity of fluid inclusions in hydrothermal breccia pipe matrix minerals (Skewes *et al.*, 2002), are other factors that enhance the solubility of Cu and S in the magmas near the roof of the chamber (Luhr, 1990).

The magmas that formed the anhydrite-bearing igneous rocks at El Teniente were also highly oxidized, as indicated by both their high ratios of sulfates to sulfides and the presence of primary magmatic hematite. Recharge of a magma chamber by hydrous, oxidized, mantle-derived mafic arc magmas (Fig. 11) has been suggested as the source of S in the case of other S-rich anhydrite-bearing igneous rocks (Hattori, 1993; de Hoog *et al.*, 2004), as well as for the large quantity of S in other large Cu deposits (Streck & Dilles, 1998; Hattori & Keith, 2001).

Lamprophyre dikes ($3{\cdot}85 \pm 0{\cdot}18$ to $2{\cdot}9 \pm 0{\cdot}6$ Ma)

The Pliocene post-mineralization lamprophyre dikes represent the last phases of igneous activity within the Teniente deposit. Mg-olivine phenocrysts and high MgO, Ni and Cr contents imply a mantle origin for the more mafic lamprophyre dikes (Stern *et al.*, 2010). Petrologically similar lamprophyres are found in the Mexican volcanic belt, and considered to be the mantle-derived parent for the more typical porphyritic hornblende andesites that form the large central-vent stratovolcanoes in this belt (Carmichael, 2002). Experimental studies suggest that the phenocryst mineral assemblages of these Mexican lamprophyres, which are identical to those from the vicinity of Teniente, imply >6 wt % dissolved water in the lamprophyre magmas (Moore & Carmichael, 1998; Blatter & Carmichael, 2001). This is consistent with a minimum of >5·2 wt % water in olivine-bearing Mexican magmas as implied by the water content of melt inclusions in olivine (Cervantes & Wallace, 2003). Carmichael (2002) suggested that between 6 wt % (the minimum to reproduce the phenocryst mineral assemblage) and 16 wt % (the maximum to saturate the mantle-derived magma at 10 kbar pressure) water, derived from the subducted oceanic lithosphere, was present in the Mexican lamprophyres. Thus we conclude that the post-mineralization lamprophyre dikes in the vicinity of El Teniente imply a significant temporal increase in the extent of hydration of the sub-Andean mantle below this region between the Late Miocene and the Pliocene.

The higher Sr and La/Yb, and the lower Y and Yb of the Pliocene lamprophyres compared with the Late Miocene basaltic rocks of the Teniente Volcanic and Plutonic Complex (Stern *et al.*, 2010) suggest both a lower degree of mantle partial melting and/or a greater proportion of either garnet or hornblende in the mantle source of the lamprophyres. A lower degree of partial melting is consistent with the much smaller volume of Pliocene compared with Late Miocene igneous rocks in the vicinity of Teniente (Stern & Skewes, 2005), and hornblende in the mantle source is consistent with both the presence of hornblende phenocrysts in the most mafic olivine-bearing dikes and the extensive hydration of their source as implied by the results of the experimental studies described above. Carmichael (2002) suggested that the source of Mexican lamprophyres is metasomatized mantle containing amphibole, similar to the mineralogy of the hornblende-lherzolite mantle xenoliths observed (Blatter & Carmichael, 1998).

Significantly, the less mafic, olivine-free lamprophyre dikes have similar or higher La, but lower Yb, resulting in significantly higher La/Yb compared with the mafic lamprophyres (Stern *et al.*, 2010). We suggest that this is the product of amphibole fractionation, as heavy REE are compatible in amphibole and amphibole is the most abundant observed phenocryst in these lamprophyres. Nearly constant Dy/Yb ratios (2·0–2·3) for lamprophyres that vary between 50·3 and 61·1 wt % SiO_2 are also consistent with crystal–liquid fractionation involving amphibole rather than garnet (Davidson *et al.*, 2007). Nearly constant Sr contents in the less mafic compared with the more mafic lamprophyres, and the lack of a negative Eu anomaly, also indicate that plagioclase was not a significant fractionating crystal phase, consistent with it not being a phenocryst phase. However, the lack of plagioclase fractionation was due to the high H_2O content of the lamprophyre magma, which suppresses plagioclase crystallization and enhances the extent of amphibole crystallization, and not due to stabilization of garnet at the expense of plagioclase caused by high pressure in the magma source or crystal-fractionation region as suggested by Kay *et al.* (2005). Garnet may have existed in the mantle-source region of the mafic lamprophyres, but we consider the trend to higher La/Yb and lower Yb observed between the more and less mafic samples to be due to crystal fractionation involving amphibole and not to garnet fractionation. This reflects the increased importance of water in the mantle source of these rocks, and not an increase in the depth of magma generation or subsequent differentiation.

Regional temporal isotopic evolution

Previous regional studies of igneous rocks at the latitude of El Teniente documented significant changes in the isotopic compositions of magmas formed during the final stages of the Oligocene to Pliocene magmatic episode in the vicinity of the Teniente deposit (Figs 5 and 6; Stern & Skewes, 1995; Nystrom *et al.*, 2003; Kay *et al.*, 2005). These reflect temporal changes in the isotopic composition of the source region of these Andean magmas, involving increasing $^{87}Sr/^{86}Sr$ and decreasing $^{143}Nd/^{144}Nd$, that are interpreted to indicate a progressive increase in the amount of crustal components incorporated into the Andean magmas through time.

Our data indicate that the isotopic changes to higher $^{87}Sr/^{86}Sr$ and lower $^{143}Nd/^{144}Nd$ observed between the Early Miocene and Pliocene occurred in mantle-derived olivine-bearing mafic rocks, specifically in the sequence from olivine-basalts of the Early Miocene Coya-Machalí Formation, to olivine-basalts of the Late Miocene Teniente Mafic Complex, and finally Pliocene post-mineralization olivine-lamprophyre dikes (Stern *et al.*, 2010) and olivine-bearing basaltic andesite lavas in the Cachapoal river west of the Teniente deposit (Stern & Skewes, 1995). This trend must therefore result from isotopic variations in the sub-arc mantle and may be caused by increased mantle-source region contamination by subducted components (Stern, 1991). Stern *et al.* (2010) presented a model for Sr and Nd isotopic variations caused by different amounts of contamination of the sub-arc mantle involving subducted trench sediment containing both marine and terrigenous components as calculated by Macfarlane (1999). The model suggests that Coya Machalí magmas could form by melting of a mantle contaminated by 1% subducted sediment, the Teniente Volcanic and Plutonic Complex rocks by 2% subducted sediment, the Pliocene post-mineralization lamprophyre dikes by 4% subducted sediment, and the Late Pliocene basaltic andesite lavas in the Cachopoal river valley by 6% subducted sediment.

Kay *et al.* (2005) presented a model of assimilation of continental crust, consisting of Paleozoic–Triassic granitic basement, by a primitive Coya-Machalí olivine basalt that produces the same isotopic variations as does the source region contamination model, but with much higher proportions of assimilation: 15% to produce the Late Miocene Teniente Volcanic and Plutonic Complex rocks, 30% to produce the Pliocene lamprophyre dikes and 40% to produce the Cachopoal lavas and northern SVZ volcanic rocks. However, these amounts of assimilation of high-SiO_2, low-Sr granite are clearly inconsistent with the primitive mafic chemistry of the olivine-bearing basalts in the Teniente Mafic Complex and olivine lamprophyre dikes. Furthermore, the isotopic data, including the recently published data for O and Hf isotopes in zircons from all the felsic units in the deposit (Muñoz *et al.*, 2009), indicate that mafic, intermediate and felsic igneous rocks of each of the episodes of igneous activity in the Andes at the latitude of El Teniente, are, for each age group, isotopically similar to each other (Figs 5 and 6). These data rule out significant intra-crustal contamination or melting of isotopically heterogeneous Paleozoic and Mesozoic Andean continental crust in the generation of the rocks of each age group.

Stern (1991, 2004), Stern & Skewes (1995, 2005) and Kay *et al.* (2005) concluded, based on both geochemical arguments and structural grounds, that significant (~50 km) fore-arc truncation by subduction erosion has occurred since 9 Ma across the arc–trench gap west of El Teniente, and that an important part of the temporal isotopic changes observed in the igneous rocks generated through time at this latitude resulted from subduction erosion of the continental margin and increased contamination by continental components of the sub-arc mantle. Subduction of oceanic crust, pelagic and terrigenous sediments, and continental crust tectonically eroded off the edge of the continent, into the mantle-source region of Andean magmas, may provide the large amounts of water, sulfur, copper and boron involved in the generation of the giant copper deposits of central Chile (Macfarlane, 1999). Significantly, as discussed above, the change from olivine-basalts in the Late Miocene Teniente Mafic Complex to the isotopically distinct olivine + amphibole lamprophyre post-mineralization dikes emplaced in the Pliocene implies progressively greater hydration of the sub-arc mantle over this time period. There is thus a correlation between the increasing water content of the Andean sub-arc mantle and the increasing degree of contamination of this mantle by subducted components as indicated by the isotopic data. A similar correlation has been documented in magmas erupted from different regions of the subduction-related trans-Mexican volcanic arc (Cervantes & Wallace, 2003).

CONCLUSIONS

Lindgren & Bastin (1922) suggested that El Teniente 'affords convincing evidence of the intimate genetic connection between igneous rocks and ore deposits'. The petrochemical constraints on the genesis of the igneous rocks in the deposit provide important insights into this genetic connection. We conclude that both the magmatic–hydrothermal breccia pipes and the sequence of felsic porphyry plutons in the deposit were derived from a large, long-lived 'productive' magmatic system, one that involved at least >600 km^3 of Andean magma over an ~3 Myr period (Fig. 11). This system developed in the upper crust at a depth of at least 4 km below the surface, as indicated by the fact that the depth of the roots of the largest breccia pipes at El Teniente, which are as yet unknown, must extend down to at least this depth.

Decreasing subduction angle, compression and crustal thickening also played an important role in the generation of the El Teniente deposit. They caused the termination of volcanism, which sealed the magmatic system and allowed volatiles to build up in concentration near the roof of the system, until volatile pressure exceeded confining pressure, generating the large mineralized breccia pipes that characterize the deposit. Together they also resulted in a decrease in the volume of the sub-arc mantle and consequently an increase in the relative input of slab-derived fluids into this mantle, which was the source region of the magmas that fed and maintained the magmatic system from which the metals, mineralizing fluids and host igneous rocks were derived. The production of progressively more hydrated and oxidized magmas between the Late Miocene and the Pliocene may have facilitated the transfer of greater amounts of oxidized sulfur and metals out of the roof of the magmatic system into the shallow crust, because in less oxidized and volatile-poor systems sulfur and metal are retained near the base of the system as immiscible sulfur and pyrrhotite (Richards, 2003, 2005).

In summary, the major factor in producing the giant El Teniente deposit was the development of a large, long-lived magma chamber or magmatic plumbing system. The transfer of metals from the magma in this chamber took place by the exsolution of volatiles from the roof of this system as it crystallized, generating large mineralized breccia pipes and associated veins. Progressively more differentiated felsic intrusions, of smaller and smaller volume, also intruded into the deposit, but these truncated already altered, brecciated and mineralized rocks, and were not the major process by which Cu was emplaced into the deposit (Skewes *et al.*, 2002, 2005). These felsic porphyries have the same isotopic composition as all the more mafic lithologies associated with the deposit, and they did not form by progressively deeper melting within the isotopically heterogeneous Andean crust. They were generated instead by a complex combination of differentiation processes in the large relatively shallow magma chamber below the deposit, including recharge of the base of the chamber by mantle-derived mafic magmas, thermal stratification and convection, magma mixing and crystallization, crystal–liquid fractionation involving amphibole, bubble formation, and volatile transfer and concentration in the upper cooler parts of the chamber.

ACKNOWLEDGEMENTS

We thank Patricio Zuñiga, superintendent of geology at El Teniente, for access to and logistic support within the mine. The manuscript benefited from constructive comments from Jeremy Richards, Victor Maksaev and two anonymous reviewers. Dan Mitchell assisted with the figures.

SUPPLEMENTARY DATA

Supplementary data for this paper are available at *Journal of Petrology* online.

REFERENCES

Annen, C., Blundy, J. D. & Sparks, R. S. J. (2006). The genesis of intermediate and silica magmas in deep crustal hot zones. *Journal of Petrology* **47**, 505–539.

Atkinson, W. W., Jr, Souvirón, S., Vehrs, T. & Faunes, A. (1996). Geology and mineral zoning of the Los Pelambres porphyry copper deposit, Chile. In: Camus, F., Sillitoe, R. H. & Petersen, R. (eds) *Andean Copper Deposits. Society of Economic Geologists Special Publications* **5**, 131–155.

Bachman, O. & Bergantz, G. W. (2004). On the origin of crystal-poor rhyolites: Extracted from batholithic crystal mushes. *Journal of Petrology* **45**, 1565–1582.

Baker, M. C. W. & Francis, P. W. (1978). Upper Cenozoic volcanism in the Central Andes; ages and volumes. *Earth and Planetary Science Letters* **41**, 175–187.

Barth, A. P. & Dorais, M. J. (2000). Magmatic anhydrite in granitic rocks: first occurrence and potential petrologic consequences. *American Mineralogist* **85**, 430–435.

Blatter, D. K. & Carmichael, I. S. E. (1998). Hornblende peridotite xenoliths from central Mexico reveal the highly oxidized nature of subarc upper mantle. *Geology* **26**, 1035–1038.

Blatter, D. K. & Carmichael, I. S. E. (2001). Hydrous phase equilibria of a Mexican high-silica andesite: a candidate for mantle origin? *Geochimica et Cosmochimica Acta* **65**, 4043–4065.

Brown, S. J. A. & Fletcher, I. R. (1999). SHRIMP U–Pb dating of pre-eruption growth history of zircons from the 340 ka Whakamaru Ignimbrite, New Zealand: evidence for >250 k.y. magma residence times. *Geology* **27**, 1035–1038.

Burgos, A. (2002). Petrografía y Geoquímica de la Diabasas y Diques Basálticos que constituyen las 'Andesitas de la Mina' en el yacimiento El Teniente, VI Región, Chile. Universidad de Concepción: Memoria de Título, 108 p.

Camus, F. (1975). Geology of the El Teniente orebody with emphasis on wall-rock alteration. *Economic Geology* **70**, 1341–1372.

Cannell, J., Cooke, D., Walshe, J. L. & Stein, H. (2005). Geology, mineralization, alteration, and structural evolution of El Teniente porphyry Cu–Mo deposit. *Economic Geology* **100**, 979–1004.

Carmichael, I. S. E. (2002). The andesite aqueduct: perspectives on the evolution of intermediate magmatism in west–central (105–99°W) Mexico. *Contributions to Mineralogy and Petrology* **143**, 641–663.

Cervantes, P. & Wallace, P. (2003). The role of water in subduction zone magmatism: New insights from melt inclusions in high-Mg basalts from central Mexico. *Geology* **31**, 235–238.

Charrier, R., Baeza, O., Elgueta, S., Flynn, J. J., Gans, P., Kay, S. M., Muñoz, N., Wyss, A. R. & Zurita, E. (2002). Evidence for Cenozoic extensional basin development and tectonic inversion south of the flat-slab segment, southern Central Andes, Chile (33°–36°S.L.). *Journal of South American Earth Sciences* **15**, 117–139.

Cline, J. S. & Bodnar, R. J. (1991). Can economic porphyry copper mineralization be generated by a typical calc-alkaline melt? *Journal of Geophysical Research* **96**, 8113–8126.

Cloos, M. (2001). Bubbling magma chambers, cupulas and porphyry copper deposits. *International Geology Reviews* **43**, 285–311.

Cornejo, P., Tosdal, R. M., Mpodozis, C., Tomlinson, A. J., Rivera, O. & Fanning, C. M. (1997). El Salvador, Chile, porphyry copper

revisited: geologic and geochronologic framework. *International Geology Review* **39**, 22–54.

Cuadra, P. (1986). Geocronología K–Ar del yacimiento El Teniente y áreas adyacentes. *Revista Geológica de Chile* **27**, 3–26.

Davidson, J., Turner, S., Handley, H., Macpherson, C. & Dosseto, A. (2007). Amphibole 'sponge' in arc crust. *Geology* **35**, 787–790.

de Hoog, J. C. M., Hattori, K. H. & Hoblitt, R. P. (2004). Oxidized sulfur-rich mafic magma at Mount Pinatubo, Philippines. *Contributions to Mineralogy and Petrology* **146**, 750–761.

de Silva, S. L. (1989). The Altiplano–Puna Volcanic Complex of the Central Andes. *Geology* **17**, 1102–1106.

Farmer, G. L., Broxton, D. E., Warren, R. G. & Pickthorn, W. (1991). Nd, Sr, and O isotopic variations in metaluminous ash-flow tuffs and related volcanic rocks at the Timber Mountain/Oasis Valley Caldera Complex, SW Nevada: implications for the origin and evolution of large-volume silicic magma bodies. *Contributions to Mineralogy and Petrology* **109**, 53–68.

Floody, R. (2000). Estudio de vulnerabilidad geológica-geotecnia de Chimenea de Brecha Braden. Fase 1, Geología de Brechas Braden: Internal Report GL-044/00, Superintendencia Geología de El Teniente, CODELCO-CHILE, 90 p.

Freydier, C., Ruiz, J., Chesley, J., Candless, T. & Munizaga, F. (1997). Re–Os isotope systematics of sulfides from felsic igneous rocks: application to base metal porphyry mineralization in Chile. *Geology* **25**, 775–778.

Frikken, P. H., Cooke, D. R., Walshe, J. L. & Archibald, D. (2005). Mineralogical and isotopic zonation in the Sur-Sur tourmaline breccia, Río Blanco–Los Bronces Cu–Mo deposit, Chile. *Economic Geology* **100**, 935–961.

Garrido, I., Cembrano, J., Siña, A., Stedman, P. & Yáñez, G. A. (2002). High magma oxidation state and bulk crustal shortening: key factors in the genesis of Andean porphyry copper deposits, central Chile (31–34°S). *Revista Geológica de Chile* **29**, 43–54.

Giambiagi, L. B. & Ramos, V. A. (2002). Structural evolution of the Andes in a transitional zone between flat and normal subduction (33°300–33°450S), Argentina and Chile. *Journal of South American Science* **15**, 101–116.

Giambiagi, L. B., Tunik, M. & Ghiglione, M. (2001). Cenozoic tectonic evolution of the Alto Tunuyán foreland basin above the transition zone between the flat and normal subduction segment (33°300–34°000S), western Argentina. *Journal of South American Earth Sciences* **14**, 707–724.

Gill, J. (1981). *Orogenic Andesites and Plate Tectonics. Mineral, Rocks and Inorganic Materials*, **Vol. 16**, Berlin: Springer.

Godoy, E., Yáñez, G. & Vera, E. (1999). Inversion of an Oligocene volcanic–tectonic basin and uplifting of its superimposed Miocene magmatic arc in the Chilean Central Andes: first seismic and gravity evidences. *Tectonophysics* **306**, 217–236.

González, R. A. (2006). *Petrografía geoquímica y microtermometría de los intrusivos félsicos del sector norte del yacimiento El Teniente*. Universidad de Concepción: Memoria de Título, 149 p.

Guzmán, C. (1991). *Alteración y mineralización de los pórfidos dioríticos del sector central del yacimiento El Teniente*. Universidad de Chile, Santiago: Memoria de Título, 145 p.

Halliday, A. N., Mahood, G. A., Holden, P., Mertz, J. M., Dempster, T. J. & Davidson, J. P. (1989). Evidence for long residence times of rhyolitic magma in the Long Valley magmatic system: the isotopic record in precaldera lavas of Glass Mountain. *Earth and Planetary Science Letters* **94**, 274–290.

Hattori, K. (1993). High-sulfur magma, a product of fluid discharge from underlying mafic magma: Evidence from Mount Pinatubo, Philippines. *Geology* **21**, 1083–1086.

Hattori, K. H. & Keith, J. D. (2001). Contributions of mafia melt for porphyry deposits: evidence from Pinatubo and Bingham. *Mineralium Deposita* **36**, 799–806.

Hawkesworth, C. J., Blake, S., Evans, P., Hughes, R., Macdonald, R., Thomas, L. E., Turner, S. P. & Zellmer, G. (2000). Time scales of crystal fractionation in magma chambers—integrating physical, isotopic, and geochemical perspectives. *Journal of Petrology* **41**, 991–1006.

Heinrich, C. A., Halter, W., Landtwing, M. R. & Pettke, T. (2005). The formation of economic porphyry copper(–gold) deposits: Constraints from microanalysis of fluid and melt inclusions. In: McDonald, I., Boyce, A. J., Butler, I. B., Herrington, R. J. & Polya, D. A. (eds) *Mineral Deposits and Earth Evolution*, **Vol. 248**, Geological Society, London: Special Publications, pp. 247–264.

Hildreth, W., Grunder, A. L. & Drake, R. E. (1984). The Loma Seca Tuff and the Calabozos Caldera: a major ash-flow and caldera complex in the Southern Andes of Central Chile. *Geological Society of America Bulletin* **95**, 45–54.

Hitschfeld, M. E. (2006). *Petrografía y geoquímica de los intrusivos leucocráticos del sector Sur Este del yacimiento El Teniente*. Universidad de Concepción: Memoria de Título, 129 p.

Howell, F. H. & Molloy, S. (1960). Geology of the Braden orebody, Chile, South America. *Economic Geology* **70**, 863–905.

Jellinek, A. M. & DePaolo, D. J. (2003). A model for the origin of large silicic magma chambers: precursors of caldera-forming eruptions. *Bulletin of Volcanology* **65**, 363–381.

Kay, S. M., Mpodozis, C. & Coira, B. (1999). Neogene magmatism, tectonism and mineral deposits of the Central Andes (22°–33°S Latitude). In: Skinner, B. J. (ed.) *Geology and Ore Deposits of the Central Andes. Society of Economic Geologists Special Publications* **7**, 27–59.

Kay, S. M., Godoy, E. & Kurtz, A. (2005). Episodic arc migration, crustal thickening, subduction erosion, and magmatism in the south–central Andes. *Geological Society of America Bulletin* **117**, 67–88.

Klemm, L. M., Pettke, T., Heinrich, C. L. & Campos, E. (2007). Hydrothermal evolution of the El Teniente deposit, Chile: porphyry Cu–Mo ore deposition from low-salinity magmatic fluids. *Economic Geology* **102**, 1021–1045.

Koyaguchi, T. & Kaneko, K. (1999). A two-stage evolution of magmas in the continental crust. *Journal of Petrology* **40**, 241–254.

Kurtz, A. C., Kay, S. M., Charrier, R. & Farrar, E. (1997). Geochronology of Miocene plutons and exhumation history of the El Teniente region, Central Chile (34–35°S). *Revista Geológica de Chile* **16**, 145–162.

Kusakabe, M., Hori, M., Nakagawa, S., Matsuhisa, Y., Ojeda, J. M. & Serrano, L. M. (1984). Oxygen and sulfur isotopic compositions of quartz, anhydrite and sulfide minerals from the El Teniente and Río Blanco porphyry copper deposits, Chile. *Bulletin of the Geological Survey of Japan* **35**, 583–614.

Kusakabe, M., Hori, M. & Matsuhisa, Y. (1990). Primary mineralization–alteration of the El Teniente and Río Blanco porphyry copper deposits, Chile; stable isotope, fluid inclusion and Mg^{+2}/Fe^{+2}/Fe^{+3} ratios of hydrothermal fluids. In: Herbert, H. K. & Ho, S. E. (eds) Stable Isotopes and Fluid Processes in Mineralization. Perth: University of Western Australia Press, pp. 244–259.

Lindgren, W. & Bastin, E. S. (1922). Geology of the Braden mine, Rancagua, Chile. *Economic Geology* **17**, 75–99.

Luhr, J. F. (1990). Experimental phase relations of water- and sulfur-saturated arc magmas and the 1982 eruption of El Chichón volcano. *Journal of Petrology* **31**, 781–801.

Macfarlane, A. W. (1999). Isotopic studies of northern Andean crustal evolution and ore metal sources. In: Skinner, B. J. (ed.) *Geology and*

Ore Deposits of the Central Andes. Society of Economic Geologists Special Publications **7**, 195–217.

Maksaev, V. & Zentilli, M. (1988). Marco metalogenico regional de los megadepositos de tipo porfido cuprifero del norte grande de Chile. *Proceedings V Congreso Geológico Chileno, Santiago* **1**, B181–B212.

Maksaev, V., Munizaga, F., McWilliams, M., Fanning, M., Marther, R., Ruiz, J. & Zentilli, M. (2004). Chronology for El Teniente, Chilean Andes, from U–Pb, $^{40}Ar/^{39}Ar$, Re–Os, and fission track dating: implications for the formation of a supergiant porphyry Cu–Mo deposit. In: Sillitoe, R. H., Perelló, J. & Vidal, C. E. (eds) *Andean Metallogeny: New Discoveries, Concepts and Updates. Society of Economic Geologists Special Publications* **11**, 15–54.

Montecinos, P., Schärer, U., Vergara, M. & Aguirre, L. (2008). Lithospheric origin of Oligocene–Miocene magmatism in Central Chile: U–Pb ages and Sr–Pb–Hf isotope composition of minerals. *Journal of Petrology* **49**, 555–580.

Moore, G. M. & Carmichael, I. S. E. (1998). The hydrous phase equilibra (to 3 kbar) of an andesite and basaltic andesite from Western Mexico: constraints on water content and conditions of phenocrysts growth. *Contributions to Mineralogy and Petrology* **130**, 304–319.

Morel, R. & Spröhnle, C. (1992). *Mapa de la geología distrital, Hoja Sewell. Map GL88-7548.* Rancagua: Superintendencia Geología de El Teniente, CODELCO-CHILE.

Muñoz, M., Fuentes, F., Vergara, M., Aguirre, L. & Nyström, J. O. (2006). Abanico East Formation: petrology and geochemistry of volcanic rocks behind the Cenozoic arc front in the Andean Cordillera, central Chile (33°50′S). *Revista Geológica de Chile* **33**, 109–140.

Muñoz, M., Charrier, R., Maksaev, V., Fanning, M. & Deckart, K. (2009). Source constraints of the El Teniente porphyry Cu–Mo magmas: Hf–O isotopic composition from single zircon crystals. *Resumenes Expandido XII Congreso Geológico Chileno, Santiago* pp. S11–11.

Nystrom, J., Vergara, M., Morata, D. & Levi, B. (2003). Tertiary volcanism during extension in the Andean foothills of central Chile (33°15′–33°45′S). *Geological Society of America Bulletin* **115**, 1523–1537.

Oyarzún, R., Márques, A., Lillo, J., López, I. & Rivera, S. (2001). Giant versus small copper deposits of Cenozoic age in northern Chile: adakite versus normal calc-alkaline magmatism. *Mineralium Deposita* **36**, 794–798.

Pasteris, J. D. (1996). Mount Pinatubo volcano and 'negative' porphyry copper deposits. *Geology* **24**, 1075–1078.

Puig, A. (1988). Geologic and metallogenic significance of the isotopic composition of lead in galenas of the Chilean Andes. *Economic Geology* **83**, 843–858.

Rabbia, O. M., Hernández, L. B., French, D. H., King, R. W. & Ayers, J. C. (2009). The El Teniente Cu–Mo deposit from a hydrothermal rutile perspective. *Mineralium Deposita* **44**, 849–866.

Reich, M. H. (2001). *Estudio petrográfico, mineraloquímico y geoquímico de los cuerpos intrusivos de Sewell y La Huifa, yacimiento El Teniente, VI Región, Chile.* Universidad de Concepción: Memoria de Título, 111 p.

Reid, M. R., Coath, C. D., Harrison, T. M. & McKeegan, K. D. (1997). Prolonged residence times for the youngest rhyolites associated with Long Valley Caldera: $^{230}Th–^{238}U$ microprobe dating of young zircons. *Earth and Planetary Science Letters* **150**, 27–39.

Richards, J. P. (2003). Tectonic–magmatic precursors for porphyry Cu–(Mo–Au) deposit formation. *Economic Geology* **96**, 1515–1533.

Richards, J. P. (2005). Cumulative factors in the generation of giant calc-alkaline porphyry Cu deposits. In: Porter, T. M. (ed.) *Super Porphyry Copper and Gold Deposits—A Global Perspective*, **Vol. 1**, Adelaide: PGC Publishing, pp. 7–26.

Richards, J. P. & Kerrich, R. (2007). Adakite-like rocks: Their diverse origins and questionable role in metallogenesis. *Economic Geology* **102**, 537–576.

Richards, J. P., Boyce, A. J. & Pringle, M.S. (2001). Geological evolution of the Escondida area, northern Chile: A model for spatial and temporal localization of porphyry Cu mineralization. *Economic Geology* **96**, 271–305.

Rivano, S., Godoy, E., Vergara, M. & Villaroel, R. (1990). Redefinición de la Formación Farellones en la Cordillera de los Andes de Chile Central (32–34°S). *Revista Geológica de Chile* **17**, 205–214.

Rosenbaum, G., Giles, D., Saxon, M., Betts, P. G., Weinberg, R. F. & Duboz, C. (2005). Subduction of the Nazca Ridge and the Inca Plateau: Insights into the formation of ore deposits in Perú. *Earth and Planetary Science Letters* **239**, 18–22.

Sasaki, A., Ulriksen, E., Sato, K. & Ishihara, S. (1984). Sulfur isotope reconnaissance of porphyry copper and manto-type deposits in Chile and the Philippines. *Bulletin of the Geological Survey of Japan* **35**, 615–622.

Scaillet, B. & Evans, B.W. (1999). The 15 June 1991 eruption of Mount Pinatubo. I. Phase equilibria and pre-eruption $P–T–fO_2–fH_2O$ conditions of the dacite magma. *Journal of Petrology* **40**, 381–411.

Serrano, L., Vargas, R., Stambuk, V., Aguilar, C., Galeb, M., Holmgren, C., Contreras, A., Godoy, S., Vela, I., Skewes, M. A. & Stern, C. R. (1996). The late Miocene to early Pliocene Río Blanco–Los Bronces copper deposit, central Chilean Andes. In: Camus, F., Sillitoe, R. H. & Petersen, R. (eds) *Andean Copper Deposits. Society of Economic Geologists Special Publications* **5**, 120–129.

Shinohara, H., Kazahaya, K. & Lowenstern, J. B. (1995). Volatile transport in a convective magma column: Implications for porphyry mineralization. *Geology* **23**, 1091–1094.

Skewes, M. A. & Arévalo, A. (2000). El complejo de gabros y diabasas que hospedan a las Brechas mineralizadas del depósito de cobre El Teniente, Chile Central. *Resumenes Expandido IX Congreso Geológico Chileno, Puerto Varas* **1**, 380–384.

Skewes, M. A. & Holmgren, C. (1993). Solevantamiento Andino, erosión y emplazamiento de brechas mineralizadas en el depósito de cobre porfídico Los Bronces, Chile Central (33°S): aplicación de termometría de inclusiones fluidas. *Revista Geológica de Chile* **20**, 71–84.

Skewes, M. A. & Stern, C. R. (1994). Tectonic trigger for the formation of late Miocene Cu-rich breccia pipes in the Andes of central Chile. *Geology* **22**, 551–554.

Skewes, M. A. & Stern, C. R. (1995). Genesis of the giant Late Miocene to Pliocene copper deposits of central Chile in the context of Andean magmatic and tectonic evolution. *International Geology Review* **37**, 71–84.

Skewes, M. A. & Stern, C. R. (1996). Late Miocene mineralized breccias in the Andes of central Chile: Sr- and Nd-isotopic evidence for multiple magmatic sources. In: Camus, F., Sillitoe, R. H. & Petersen, R. (eds) *Andean Copper Deposits. Society of Economic Geologists Special Publications* **5**, 119–130.

Skewes, M. A. & Stern, C. R. (2007). Geology, mineralization, alteration and structural evolution of the El Teniente Porphyry Cu–Mo deposit.—A discussion. *Economic Geology* **102**, 1165–1171.

Skewes, M. A., Arévalo, A., Floody, R., Zuñiga, P. & Stern, C. R. (2002). The giant El Teniente breccia deposit: hypogene copper distribution and emplacement. In: Goldfarb, R. J. & Nielson, R. L. (eds) *Global Exploration 2002: Integrated Methods of Discovery. Society of Economic Geologists Special Publications* **9**, 299–332.

Skewes, M. A., Arévalo, A., Floody, R., Zuñiga, P. & Stern, C. R. (2005). The El Teniente megabreccia deposit, the world's largest copper deposit. In: Porter, T. M. (ed.) *Super Porphyry Copper and*

Gold Deposits—A Global Perspective, **Vol. 1**, Adelaide: PGC Publishing, pp. 83–114.

Skewes, M. A., Holmgren, C. & Stern, C. R. (2003). The Donoso copper-rich, tourmaline-bearing breccia pipe in central Chile: petrologic, fluid inclusion and stable isotope evidence for an origin from magmatic fluids. *Mineralium Deposita* **38**, 2–21.

Stanton, R. L. (1994). *Ore Elements in Arc Lavas*. Oxford: Clarendon Press.

Stern, C. R. (1989). Pliocene to present migration of the volcanic front, Andean Southern Volcanic Zone. *Revista Geológica de Chile* **16**, 145–162.

Stern, C. R. (1991). Role of subduction erosion in the generation of Andean magmas. *Geology* **19**, 78–81.

Stern, C. R. (2004). Active Andean volcanism: its geologic and tectonic setting. *Revista Geológica de Chile* **31**, 161–208.

Stern, C. R. & Skewes, M. A. (1995). Miocene to present magmatic evolution at the northern end of the Andean Southern Volcanic Zone, central Chile. *Revista Geológica de Chile* **22**, 261–272.

Stern, C. R. & Skewes, M. A. (2005). Origin of giant Miocene and Pliocene Cu–Mo deposits in Central Chile: Role of ridge subduction, decreased subduction angle, subduction erosion, crustal thickening and long-lived, batholiths-size, open system magma chambers. In: Porter, T. M. (ed.) *Super Porphyry Copper and Gold Deposits—A Global Perspective*, **Vol. 1**, Adelaide: PGC Publishing, pp. 65–82.

Stern, C. R., Amini, H., Charrier, R., Godoy, E., Hervé, F. & Varela, J. (1984). Petrochemistry and age of rhyolitic pyroclastics flows which occur along the drainage valleys of the Río Maipo and Río Cachapoal (Chile) and the Río Chaucha and Río Papagayos (Argentina). *Revista Geológica de Chile* **23**, 39–52.

Stern, C. R., Funk, J. A., Skewes, M. A. & Arévalo, A. (2007). Magmatic anhydrite in plutonic rocks at the El Teniente C–Mo deposit, Chile, and the role of sulfur- and copper-rich magmas in its formation. *Economic Geology* **102**, 1335–1344.

Stern, C. R., Floody, R. & Espiñeíra, D. (2010). Pliocene olivine–hornblende-lamprophyre dikes from Quebrada de los Sapos, El Teniente, Central Chile (34°S): Implications for the subarc mantle. *Andean Geology* **37**, (in press).

Streck, M. J. & Dilles, J. H. (1998). Sulfur evolution of oxidized arc magmas as recorded in apatite from a porphyry copper batholith. *Geology* **26**, 523–526.

Vargas, R., Gustafson, L., Vukasovic, M., Tidy, E. & Skewes, M. A. (1999). Ore breccias in the Río Blanco–Los Bronces porphyry copper deposit, Chile. In: Skinner, B. (ed.) *Geology and Ore Deposits of the Central Andes. Society of Economic Geologists Special Publications* **7**, 281–297.

Vergara, M., Charrier, R., Munizaga, F., Rivanos, S., Sepúlveda, P., Thiele, R. & Drake, R. (1988). Miocene volcanism in the Central Chilean Andes (31°30′–34°35′S). *Journal of South American Earth Sciences* **1**, 199–209.

Warnaars, F. W., Holmgren, C. & Barassi, S. (1985). Porphyry copper and Tourmaline breccias at Los Bronces–Río Blanco, Chile. *Economic Geology* **80**, 1544–1565.

Zentilli, M., Doe, B. R., Hedge, C. E., Alvarez, C., Tidy, E. & Daroca, J. A. (1988). Isótopos de plomo en yacimientos de tipo pórfido cuprífero comparados con otros depósitos metalíferos en los Andes del nortes de Chile y Argentina. *Proceedings V Congreso Geológico Chileno, Santiago* **1**, B331–B369.